GL00596

PNL-XXXX
UC-254

PARTICLE MEASUREMENT AND BRINE CHEMISTRY AT THE SALTON SEA DEEP WELL

R. J. Robertus
C. H. Kindle
R. G. Sullivan
D. W. Shannon

July 1991

Prepared for the
U.S. Department of Energy
Under Contract DE-AC06-76RLO 1830

Pacific Northwest Laboratory
Richland, Washington 99352

SUMMARY AND CONCLUSIONS

The Advanced Brine Chemistry Project, a part of the U.S. Department of Energy's Geothermal Energy Program, is addressing operating problems associated with scaling and corrosion at geothermal power plants. Under this project, Pacific Northwest Laboratory conducted a series of tests at the Salton Sea Deep Well, which has one of the highest solids contents in the world. The purpose of the tests was to evaluate monitoring instrumentation under field conditions and relate particulate formation to the brine chemistry. The instrumentation was evaluated under scaling geothermal conditions using two different principles: ultrasonic reflection and laser light scattering.

The following conclusions were drawn from the instrumentation testing and brine chemistry and particulate analyses:

1. Using reflected ultrasonic impulses to count (and obtain some limited size information on) suspended particles has been demonstrated for on-line application in a geothermal brine with strong scaling tendencies. Advantages include improved high-temperature durability for the transducer and improved sizing information from the reflected signal.

2. Counting and sizing particles using laser light scattering requires constant maintenance in geothermal applications.

3. Silica is the dominant scale species and appears in amounts orders of magnitude greater than other minor species such as barium sulfate.

4. The silica that formed at high temperatures and short residence times is very gelatinous and difficult to filter out of the brine.

5. Correlation of instrument readings with particle collection data was difficult because conditions on the filter (i.e., temperature, flowrate, and pressure) could not be maintained constant for long enough intervals to obtain comparable information.

CONTENTS

FIGURES

TABLES

1.0 INTRODUCTION

The Salton Sea is the highest-temperature geothermal reservoir in North America. The reservoir is located along the San Andreas Fault in the southern interior of California. The Deep Well is 10,000 ft deep and was drilled as part of a scientific effort, sponsored by the U.S. Department of Energy (DOE), to more fully understand the complex chemistry of geothermal resources.

As part of this effort, the Advanced Brine Chemistry Project, under DOE's Geothermal Energy Program, has several objectives that address operating problems associated with scaling and corrosion:

- Reduce geothermal well maintenance costs related to scale deposition.
- Reduce geothermal field surface equipment costs related to scale deposition and corrosion.
- Reduce geothermal power plant maintenance and equipment replacement costs related to scale deposition and corrosion.
- Reduce costs of surface disposal of sludge from geothermal brines.

Under the Advanced Brine Chemistry Project, Pacific Northwest Laboratory (PNL)[(a)] conducted a series of tests at the Salton Sea Deep Well to help plant designers more accurately predict the scaling tendencies of the brines. The testing was conducted during the Salton Sea Deep Well flow test in order to evaluate a brine with high scaling tendencies. Fluids produced from the well during the initial flow test were hypersaline, with 29% dissolved salts. During the test, at temperatures above 500°F, the brine rapidly deposited scale in the injection lines as it flashed and cooled.

The PNL tests were designed to evaluate monitoring instrumentation under field conditions and to relate particulate formation to the chemistry of the brine. The testing involved an ultrasonic transducer based particle counter that was able to count particles efficiently and provide some size information under the nonscaling conditions of a laboratory. The goal was to determine if this type of particle counter, with an ultrasonic transducer in direct contact

---

(a) Operated for the U.S. Department of Energy by Battelle Memorial Institute under Contract DE-AC06-76RLO 1830.

with the brine, functioned well enough to warrant further development for use under the scaling conditions of a geothermal power plant. This report contains the field test design and operation, and the results of the testing and analyses.

2.0 FIELD TEST OBJECTIVES

The main purpose of PNL's activities at Salton Sea were to evaluate instruments that could monitor suspended solids in the brine and in the plant's equipment. Specific tasks are listed below:

- Test the feasibility of online particle counting under scaling geothermal conditions using two different principles: ultrasonic reflection and laser light scattering.
- Relate suspended solids formation and growth in separator brine to time at temperature, pressure, and brine chemistry.
- Characterize the composition and total burden of the suspended solids.

3.0 TEST AND EQUIPMENT DESIGN

The experiments and experimental equipment were designed to gather particle samples just after the brine had flashed and then after a time delay comparable to that encountered in the vessels and pipelines of an operating plant. Similar equipment had been used successfully on the East Mesa and Heber geothermal fields (Robertus, Sullivan, and Shannon 1986). The plan was to gain information primarily on silica scaling, but also on other mineral species that might form scale during flashing and cooling steps. Rates of scaling and particle size information were to be determined.

Figure 3.1 shows a schematic of the experimental equipment. Figures 3.2 through 3.5 picture the setup as it existed during the approximately 8 days of testing. Because of the short time available to build the test stand, an existing piece of equipment used on the Heber geothermal field was reworked. This system used 1/4-in. valves and tubing, a size that had worked well at Heber.

Flashed brine first entered the experimental loop and then split into two streams. The first (Stream A) was filtered immediately. The second stream (Stream B) passed through a lag vessel. Delay time through the lag vessel was designed to be between 90 and 120 min. Stream B was filtered as it exited from the lag vessel.

Both brine streams were to be analyzed for particulates with continuous particle monitors and sample filters. Stream A1 was a hot stream which was to be analyzed using a laser particle detector. Stream A2 was the same brine except it was cooled to protect the transducer of the ultrasonic particle analyzer. Steam B1 out the lag vessel was filtered only, since there was no convenient way to move the laser analyzer between two sampling locations. Stream B2 was brine from the outlet of the lag vessel which again was cooled to protect the ultrasonic cell.

The original test plan was to set a brine inlet flow to the test stand and then change the temperature of the brine going to the lag vessel by using

a concentric pipe heat exchanger. This would provide information on how sub-cooling the brine affects particle sizes and amounts. For reasons discussed later, the heat exchanger could not be used.

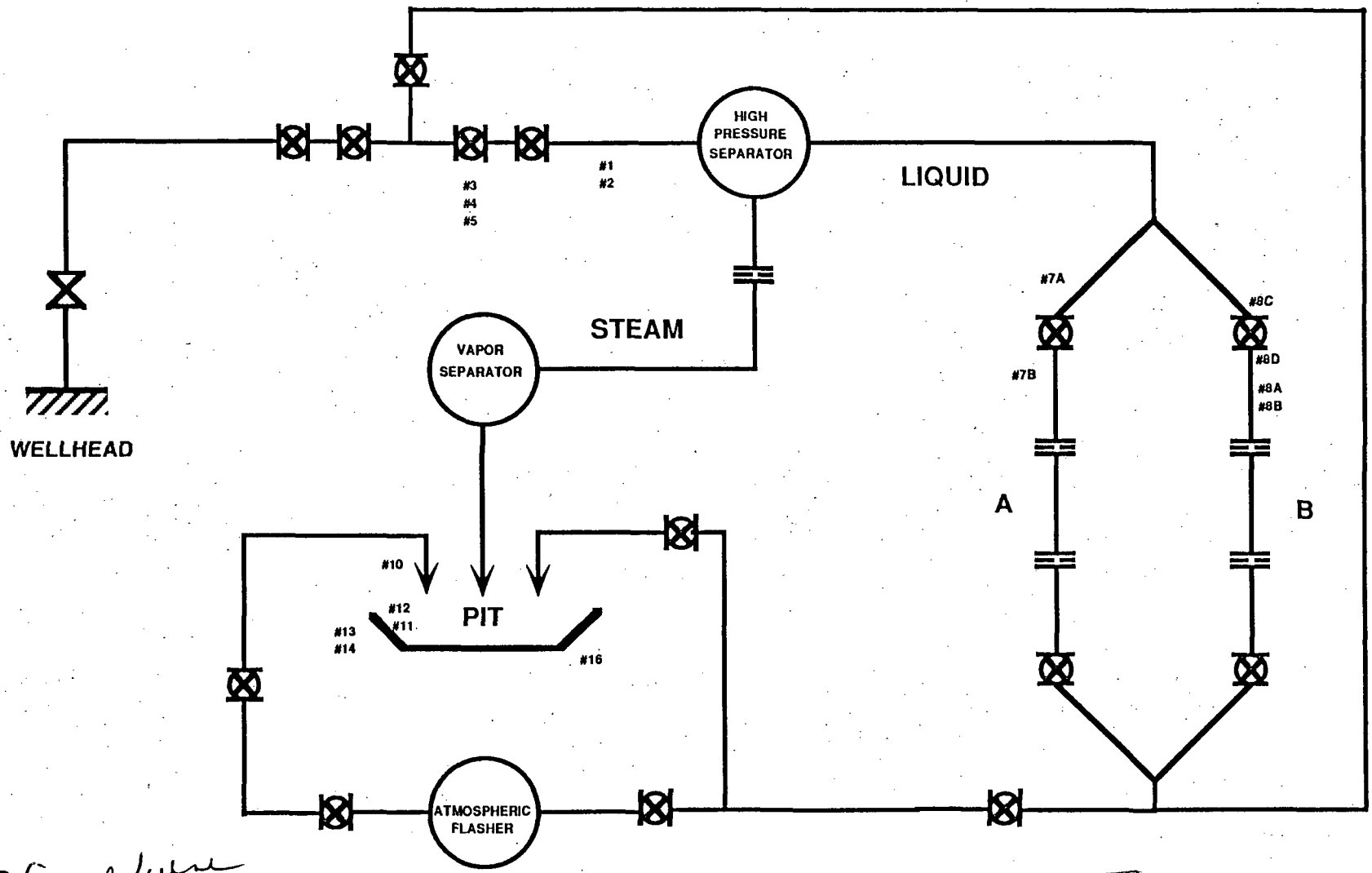

If we have had melt some distance & P,T data

FIGURE 1: TEST FACILITY STATE 2-14

PRELIMINARY DRAFT

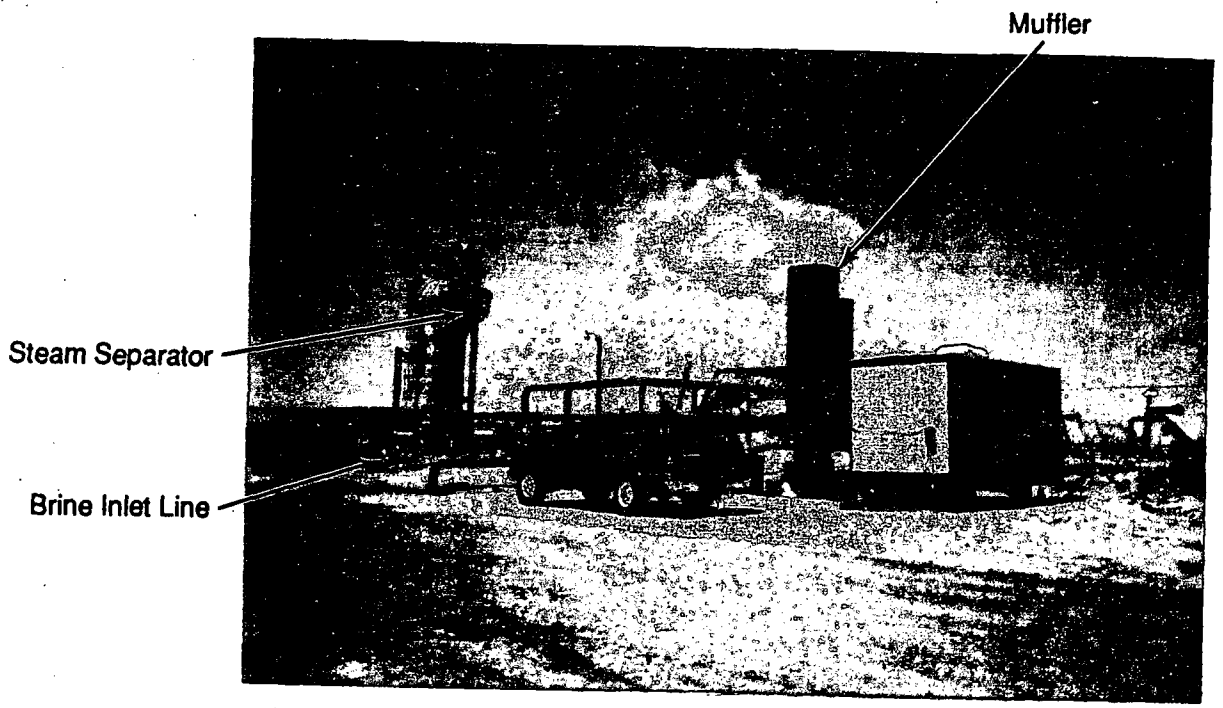

FIGURE 3.2. Salton Sea Work Site

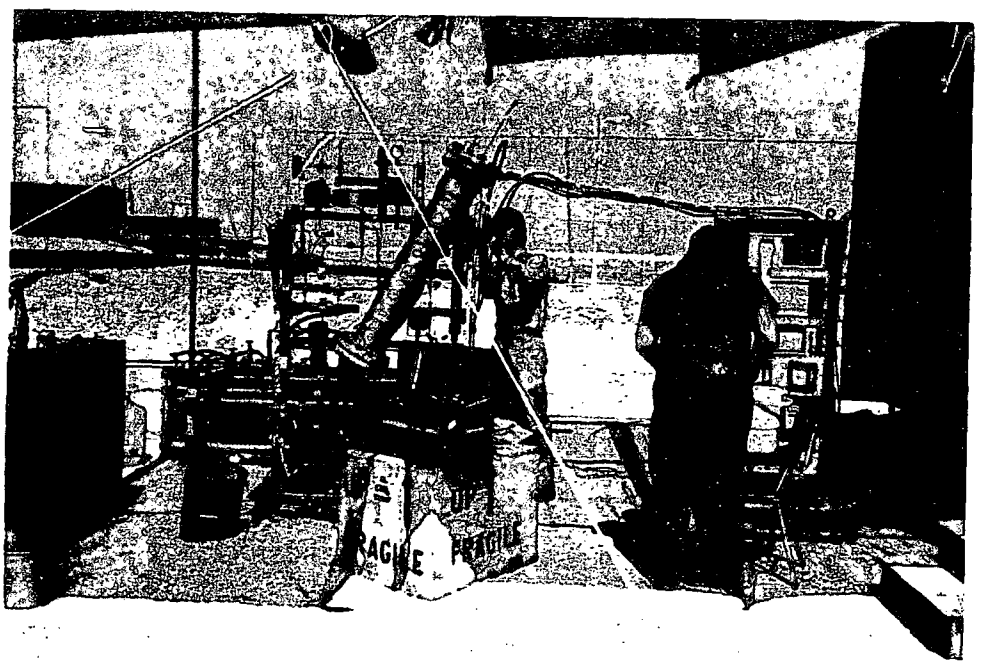

FIGURE 3.3. PNL Test Stand and Instrumentation

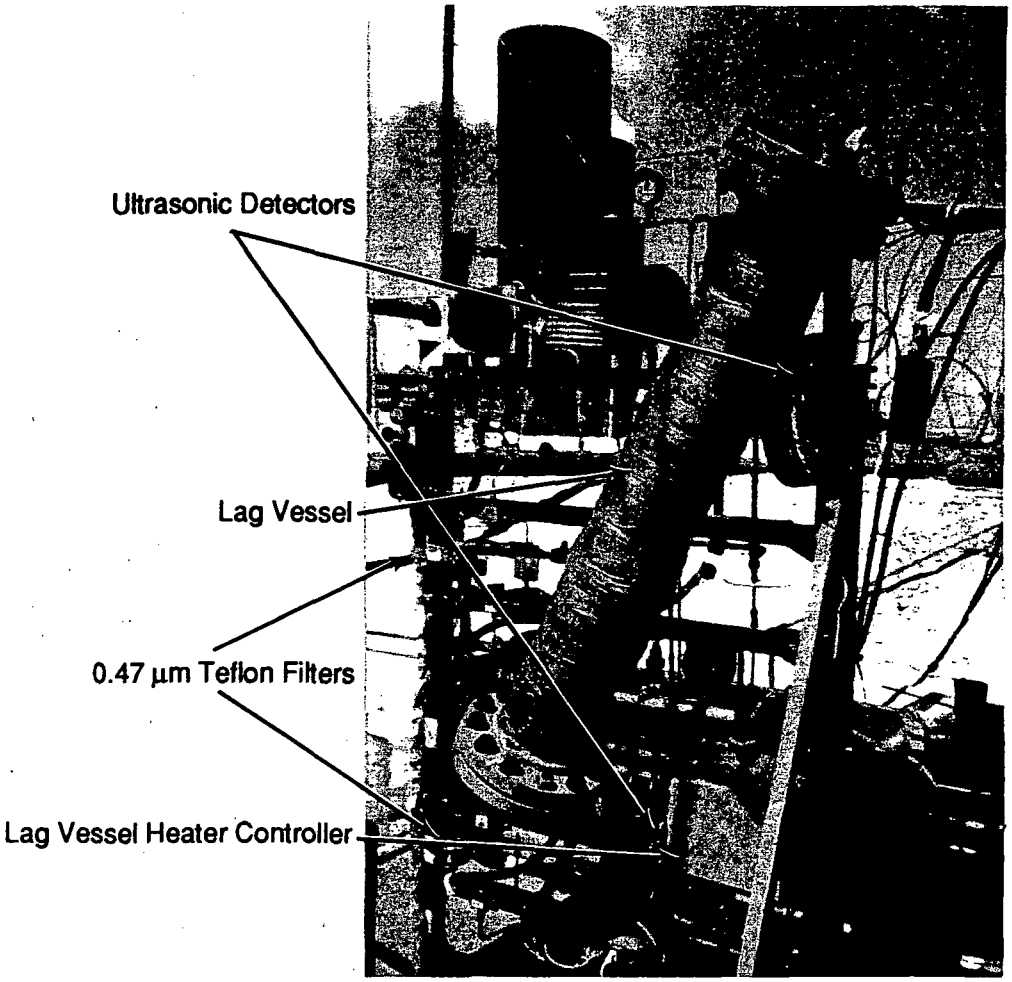

FIGURE 3.4. PNL Particle Collection Test Stand

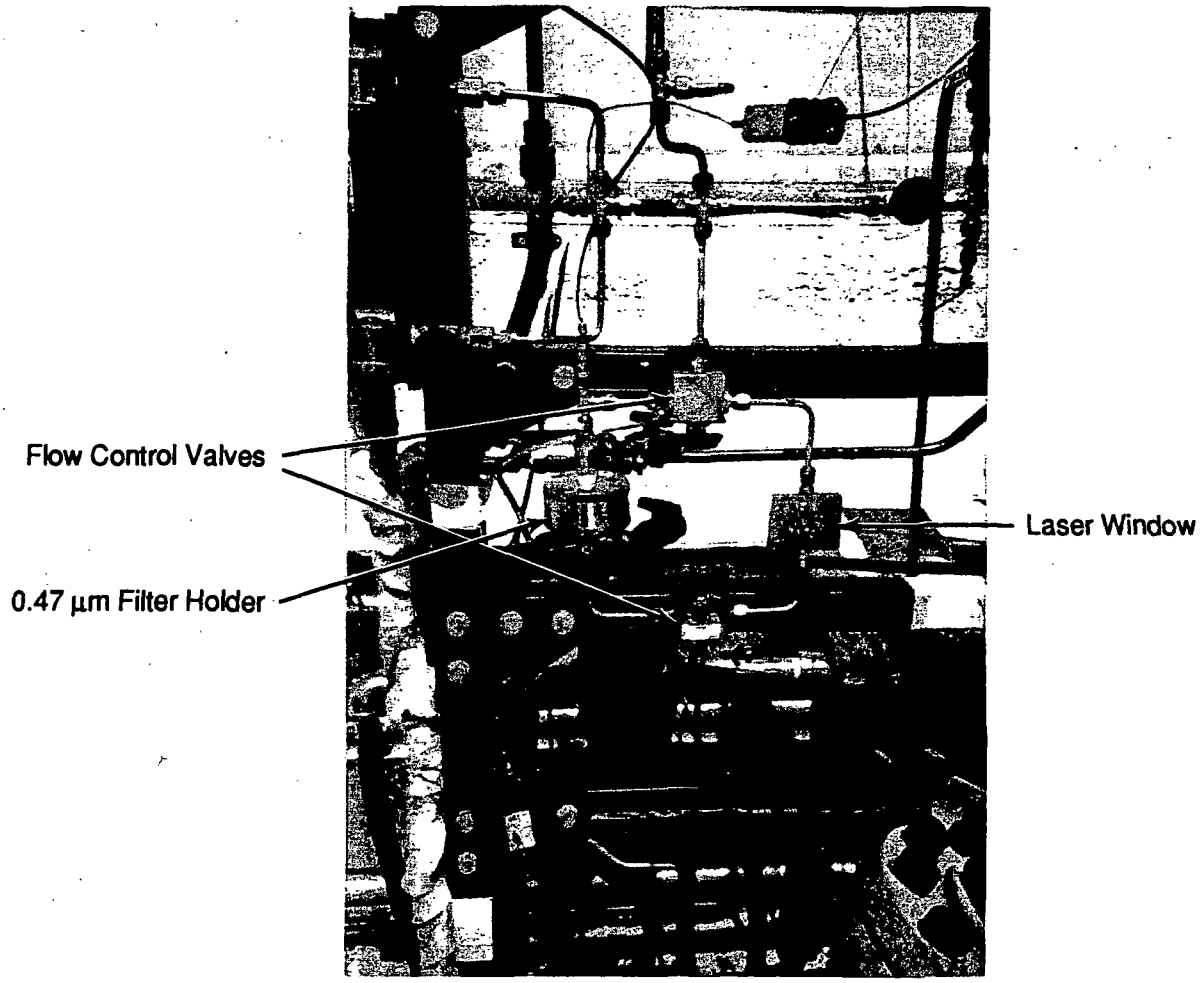

FIGURE 3.5. Detail of First Brine Path

4.0 FIELD TEST OPERATION

During May and June 1988, the site was prepared. After initial setup and checkout, the test was started on June 8 and continued until June 15. Figure 4.1 shows the times when the particle samples were taken. This particle test was just one part of a much larger DOE program to acquire production information about the well. Hence, well flow conditions to study only particle formation could not be optimized. Instead, our test was set up to sample the system at different well flow rates in order to measure effects of temperature or other changes associated with the change in flow.

The PNL test stand was located 125 ft from the main steam separator and was connected to the separator with 1/2-in. Schedule 80 pipe. A brine flow of 5 to 10 gpm was maintained in this line to reduce the residence time before measurements to about 30 s. The degree of flashing and the temperature of the brine fed to the test stand were determined by the plant operators and were dictated by the overall well-test plans in effect.

This geothermal well has one of the highest solids contents in the world. Thus, we anticipated that some scaling and plugging problems would be encountered during the test. The 20-μm filter (shown in Figure 3.1) was intended to remove large particles, but instead plugged in the first 20 min of flow and was removed for the balance of the test. With the filter out, large particles were able to get into the rest of the system and produced a number of flow interruptions. The concentric pipe heat exchanger plugged early on and was bypassed for the rest of the testing. This meant only one temperature to the lag vessel for each flashed brine (that of the brine out of the separator) could be obtained instead of four.

Under the best of conditions, the test stand ran for 3 to 4 h before lines plugged and a test was stopped. The tubing then had to be mechanically or chemically cleaned or both before the next test. Without exception, the filter on Stream A plugged within 20 min of operation. The amount of particulate collected was not always large. The precipitated silica (as determined later) appeared as a polymeric (gelatinous)-looking material, which sealed off the pores of the 0.5-μm filter paper.

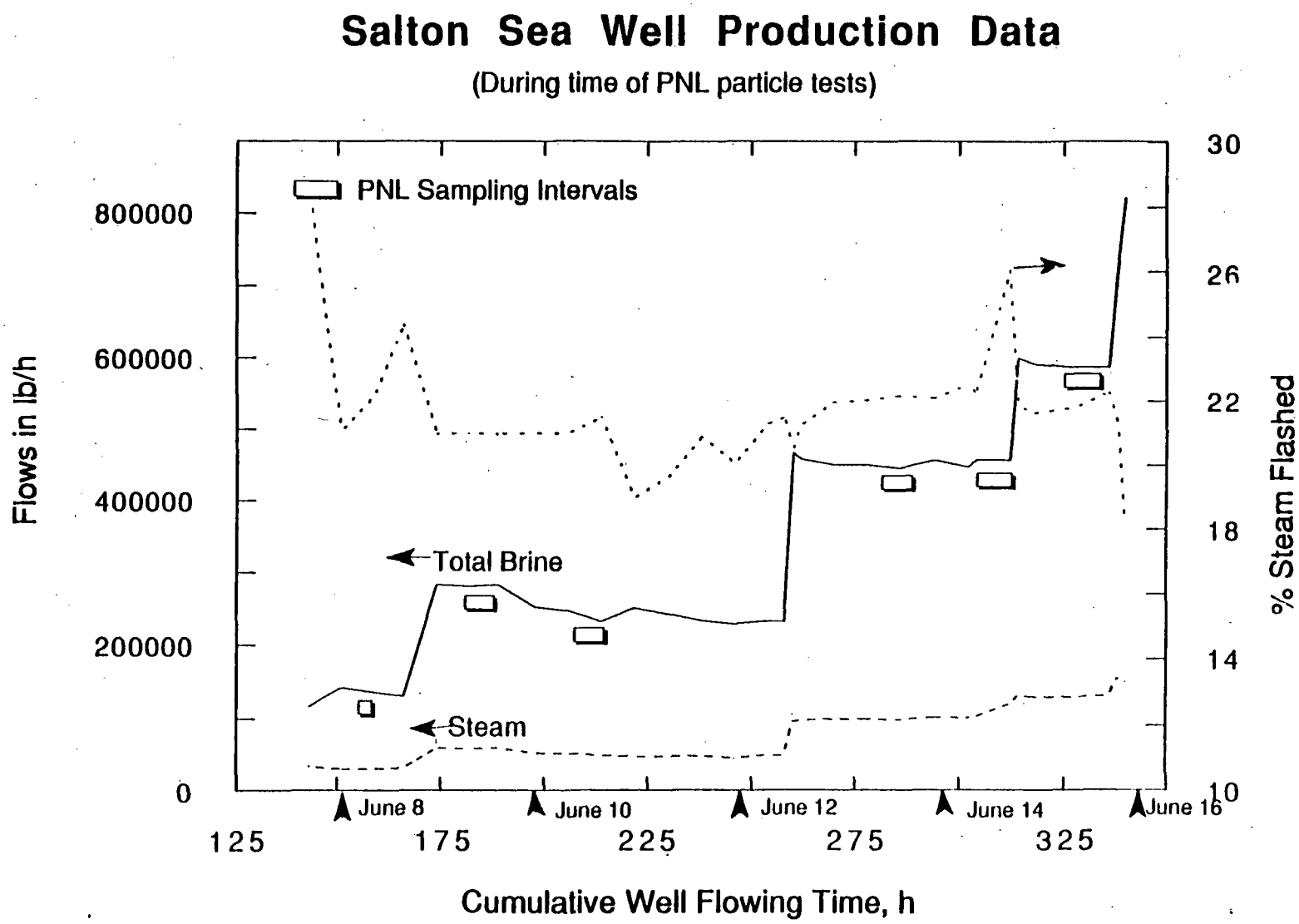

FIGURE 4.1. Well Production/Sampling Data

5.0 TEST RESULTS AND ANALYSES

This section gives the results of the instrument evaluation and analyses of brine and particle samples.

5.1 PARTICLE COUNTER EVALUATION

5.1.1 Ultrasonic Particle Counter

The ultrasonic particle counter operated successfully under severe scaling conditions and is usable in its current form by a skilled and dedicated operator. The 15 megahertz ultrasonic transducers (Figure 5.1) were installed in contact with the brine. Figure 5.2 shows the location of the transducers within the test stand. These units were remotely controlled and monitored as would be desirable in a plant location. These instruments send out a pulse, become passive, and then record the number and amplitude of reflections during a timed interval after the pulse. This timed interval (which is adjustable) makes the sensitive region correspond to a distance 2 cm into the flow. An oscilloscope was used to set the interval and power/sensitivity controls.

The instruments detected the changes in particle loading in the cooled brine (cooled to prolong transducer life). The most clear cut instances of detected particle growth were those that occurred when flow stopped and particles grew as the brine "aged" in the ultrasonic cell itself; see Figure 5.3. Figure 5.4 illustrates monitoring of the particles by the unit; both sets of data, using different thresholds, were collected at the same time by the same transducer.

There is a temperature limit of 180°F on the standard ultrasonic transducer, which was operated in the 100°F to 125°F region for this test by cooling the brine directly before the ultrasonic cell. Improvements in the electronic analysis of the reflected signals have been reported by the manufacturer through using digital signal processing units as opposed to the analog unit used in this testing.

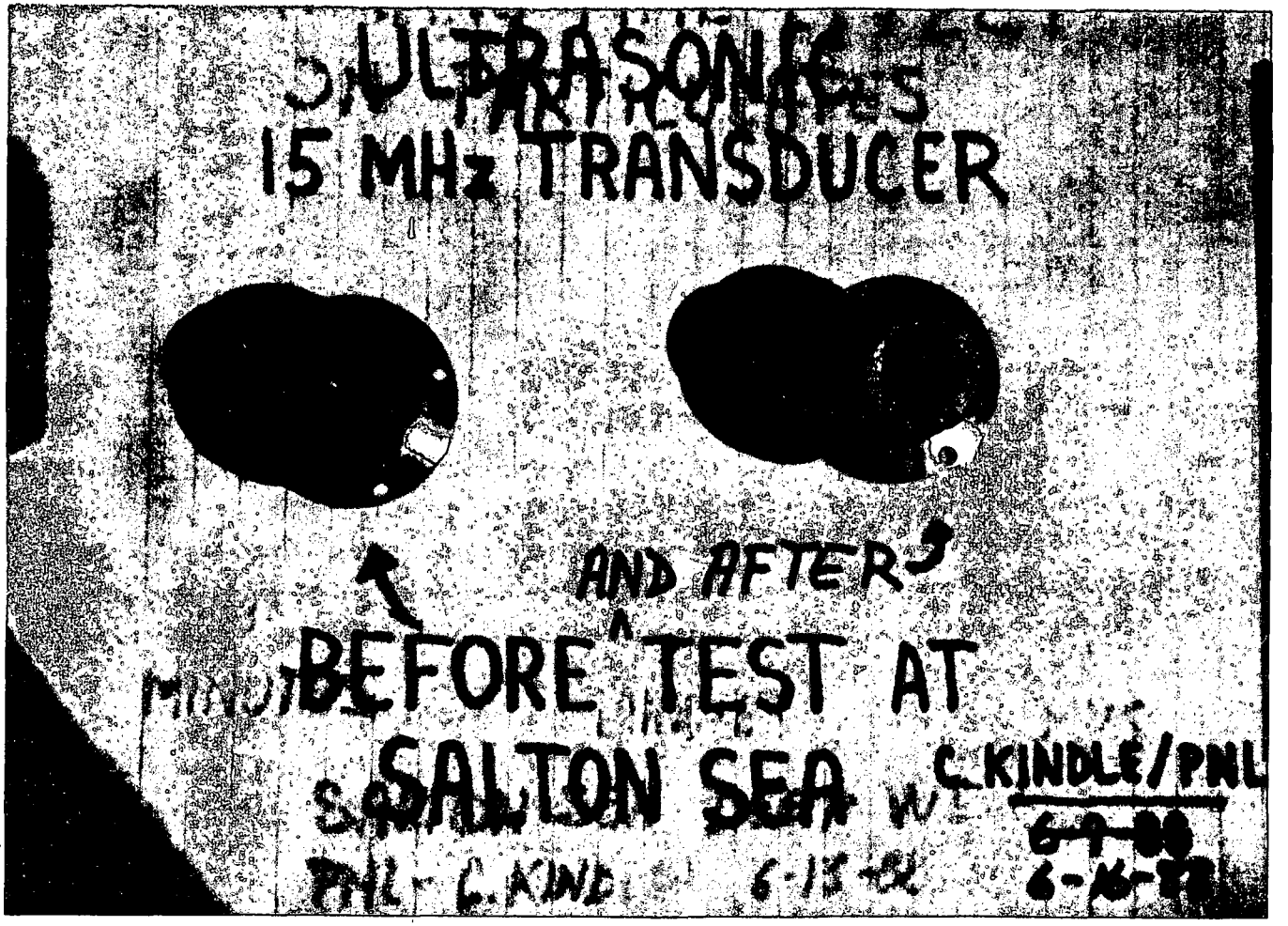

FIGURE 5.1. Ultrasonic Transducers, One After Use in the Test and One Unused, for Comparison. These were mounted with the white-tip, and the lens it encloses, in contact with the brine.

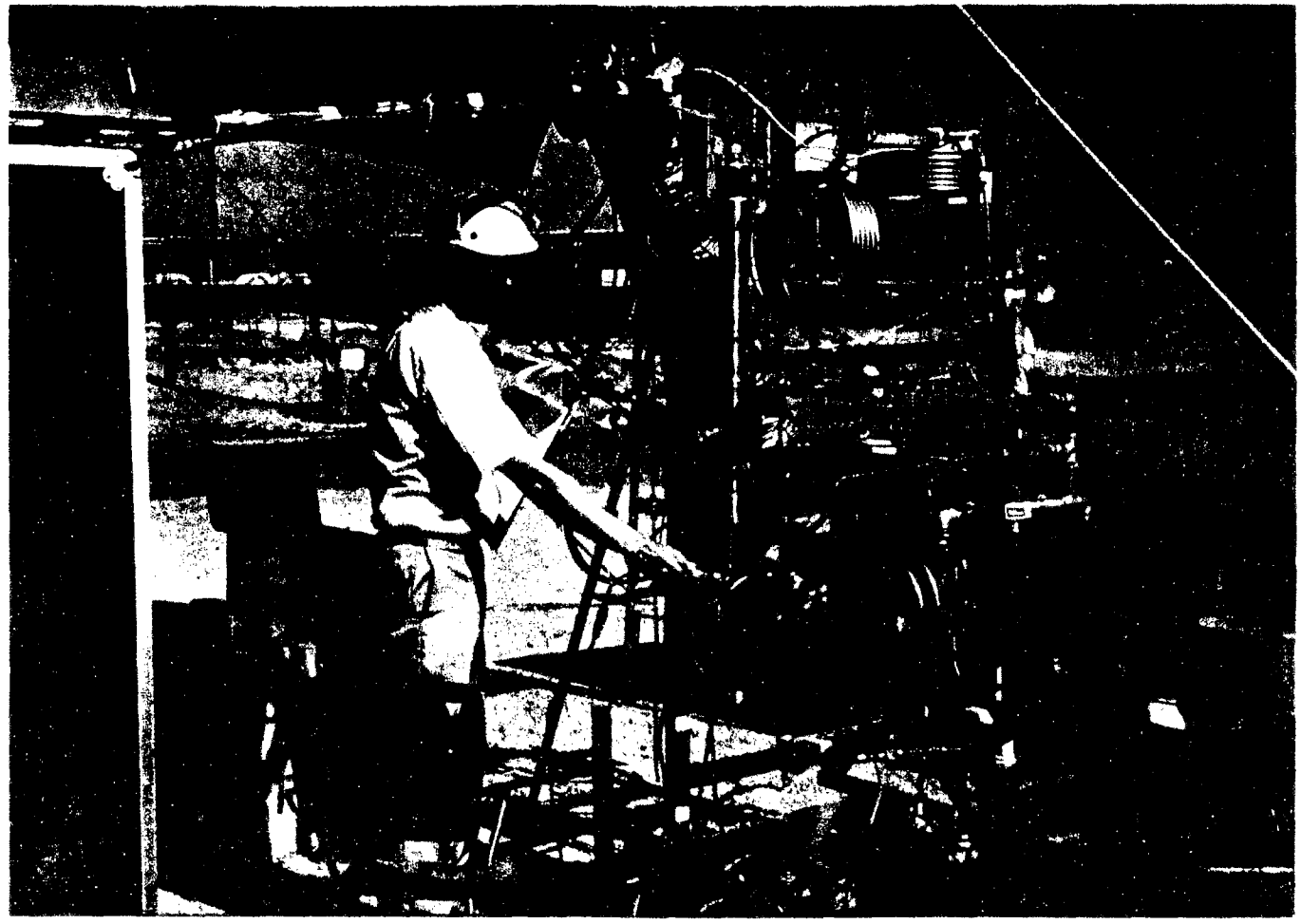

FIGURE 5.2. Ultrasonic Particle Counter Control and Data Acquisition Instruments

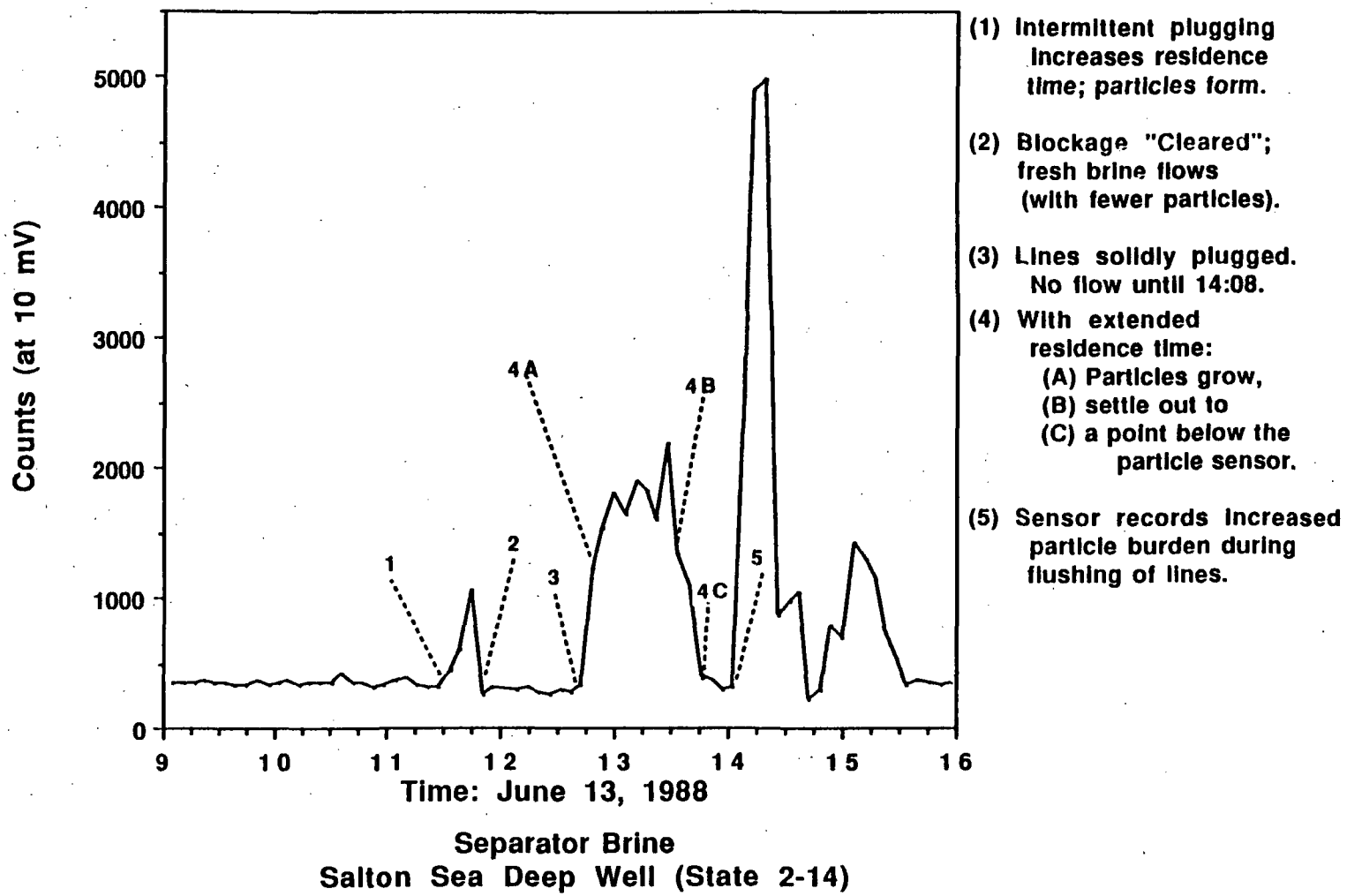

FIGURE 5.3. Ultrasonic Particle Counter Showing Particle Growth as Brine Ages

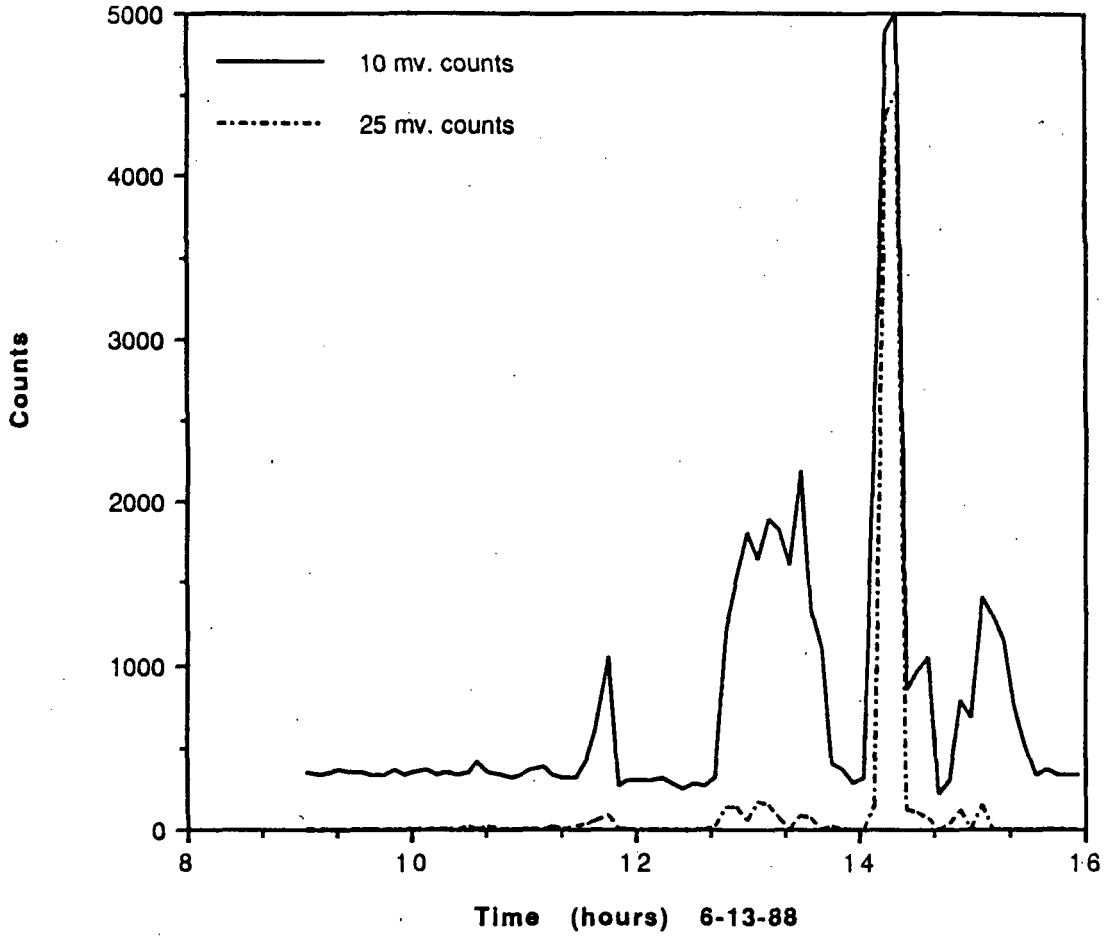

FIGURE 5.4. Comparison of Different Millivolt Thresholds on Particulate Detection Sensitivity (analog unit)

5.1.2 Laser Particle Counter

Laser particle counting operates on the principle of counting and sizing the light reflected off particulates as they pass through a cell with transparent windows. The laser window cell is thus the critical component for on-line geothermal use, and one was installed in the test loop to observe any changes after contact with this flowing brine.

The windows of the laser particle counter quickly became coated with solids (Figure 5.5) and were totally obscured in 2 days of operation. This had been recognized as a distinct possibility since window clarity had also been a problem when the laser particle counter was operated on a binary plant

(Heber), due to coating by an oily film. Thus, from tests on both flash plant and binary cycle plant brines, it is concluded that the laser light scattering approach to on-line particle counting requires continuous maintenance in geothermal applications. It will not be a suitable technique until a solution is found to keep windows transparent.

5.2 BRINE CHEMISTRY AND PARTICULATE ANALYSIS

A total of 14 brine samples and 11 particle samples were collected and returned to PNL for analysis. Table 5.1 summarizes the brine analysis data for eight samples (unfiltered). It is important to remember that the brine entering the test stand was concentrated above normal well compositions. The concentration occurred because the brine was being flashed (nominally 20% to steam), and the test stand used the bottoms fluid from the flash vessel. The decision to operate this way was made because most operating plant problems come from handling the brine after it has been flashed.

5.2.1 Brine Analyses

Figure 5.6 visually illustrates the growth of solids in the brine from the separator. This growth and precipitation of solids is a function of the brine chemistry, which is altered by the degree of flash the brine has undergone (Figure 5.7).

The solids have been qualitatively analyzed, and as expected, silica was the major constituent. Barium sulfate was also identified, and compounds of lead, arsenic, strontium, zinc, calcium, antimony, zinc, and silver were detected. Iron precipitates are present after time due to oxidation of iron. Figure 5.8 is the X-ray fluorescence analysis of the solids from the separator brine in Figure 5.7.

The brine analyses show no values for carbonate species or pH. The test stand was not designed to obtain samples that would give accurate numbers for these quantities. (Other contractors were at the site at the same time and had the responsibility for detailed brine analyses.) Sulfate analyses generally

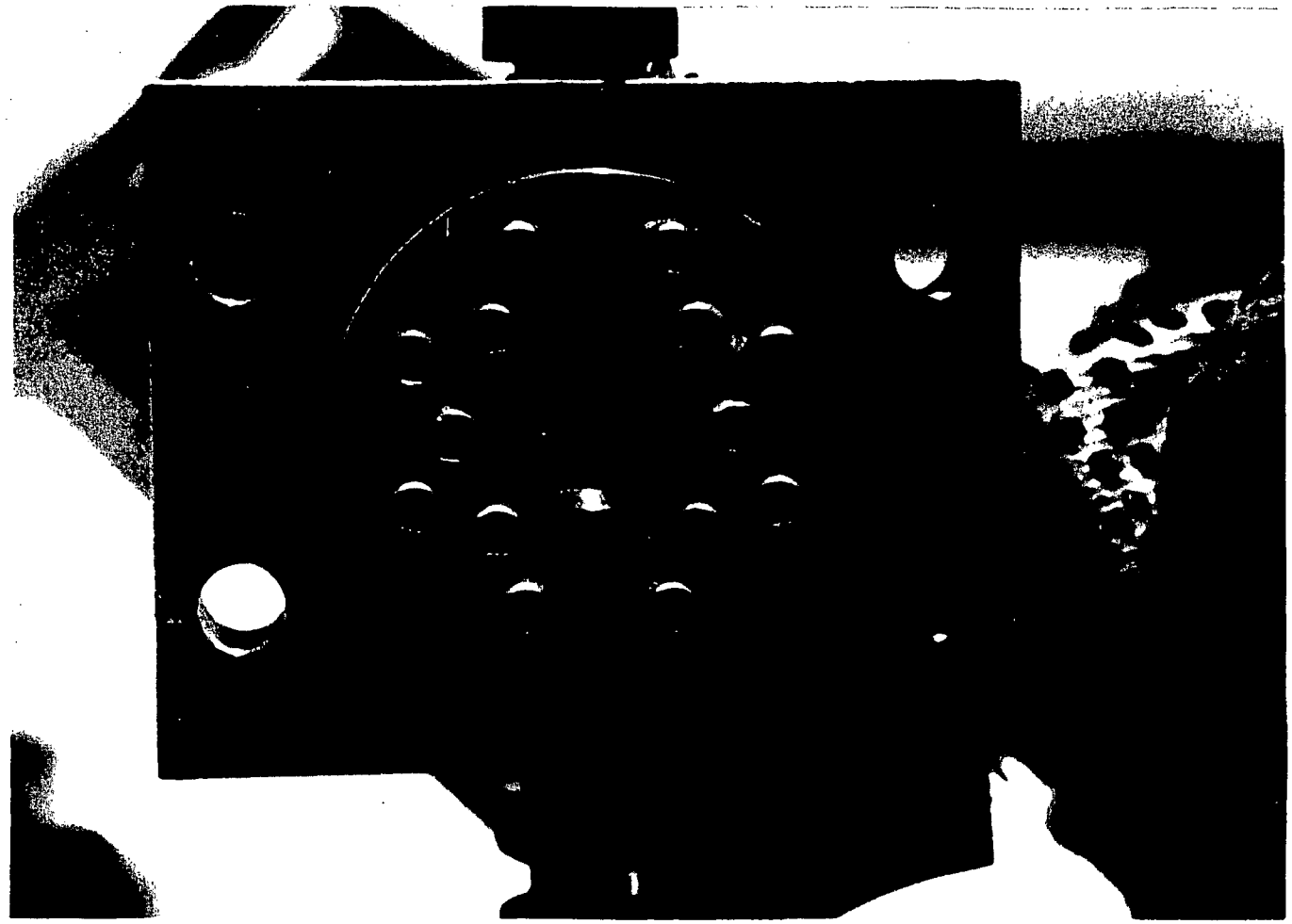

FIGURE 5.5. Laser High-Pressure Window Cell Obscured After 1 Day at the Salton Sea Well Test

TABLE 5.1. Brine Analyses Summary

Quantity Analyzed	Average Values (8 samples)	Values *.8 to Account for 20% flash	Standard Deviation of Analyzed Nos.	Deviation as % of Average	SDG&E (1980) Salton Sea Magnamax	Atomic Wts.	Millimoles/L	Moles/kgH_2O for Eq. Calcs.
Unfiltered at site								1 L = 820 g H_2O
TDS (mg/L)	361,500	289,200	12,271	3.4	183,000[a]			
pH					(5.2 at 20°C)[b]			4.7
Cl^-	199,625	159,700	10,730	5.4	112,800	35.5	4498.59	5.486
$SO_{4=}$					5.4[b]	96	5.00	0.006
CO_3^-								
HCO_3^-								
tot CO_2					(>150)[b]	44	7100.00	8.65854
Ca^{++}	37,388	29,910	2,203	5.9	19,400	40	747.75	0.91189
Cu^+	6	5	4	59.8		63.5	0.07	0.00009
Fe	1,979	1,583	136	6.9	126	58.85	26.90	0.03280
K	22,963	18,370	1,820	7.9	7,350	39	471.03	0.57442
Mg	52	42	3	5.0	97	24.3	1.72	0.00209
Na	69,650	55,720	3,698	5.3	41,700	23	2422.61	2.95440
Sr	518	414	8	1.3	393	88	4.71	0.00574
Zn	557	446	127	22.8	283	65	6.86	0.00836
As	13	10	1	10.9	(12)[b]	75	0.14	0.00017
B	462	369	12	2.6		10.8	24.19	0.04170
Ba	117	94	44	37.3	130	137.33	0.68	0.00083
Cd	2	1	0	28.5		112	0.01	0.00001
Li	328	263	16	4.7	156	6.9	38.06	0.04641
Mn	2,080	1,664	349	16.8	520	54.9	30.31	0.03696
Pb	124	100	4	2.9	21	207	0.48	0.00059
Sb						122	0.00	0.00000
SiO_2					456			

(a) Sum of average major element concentrations.
(b) White (1968).

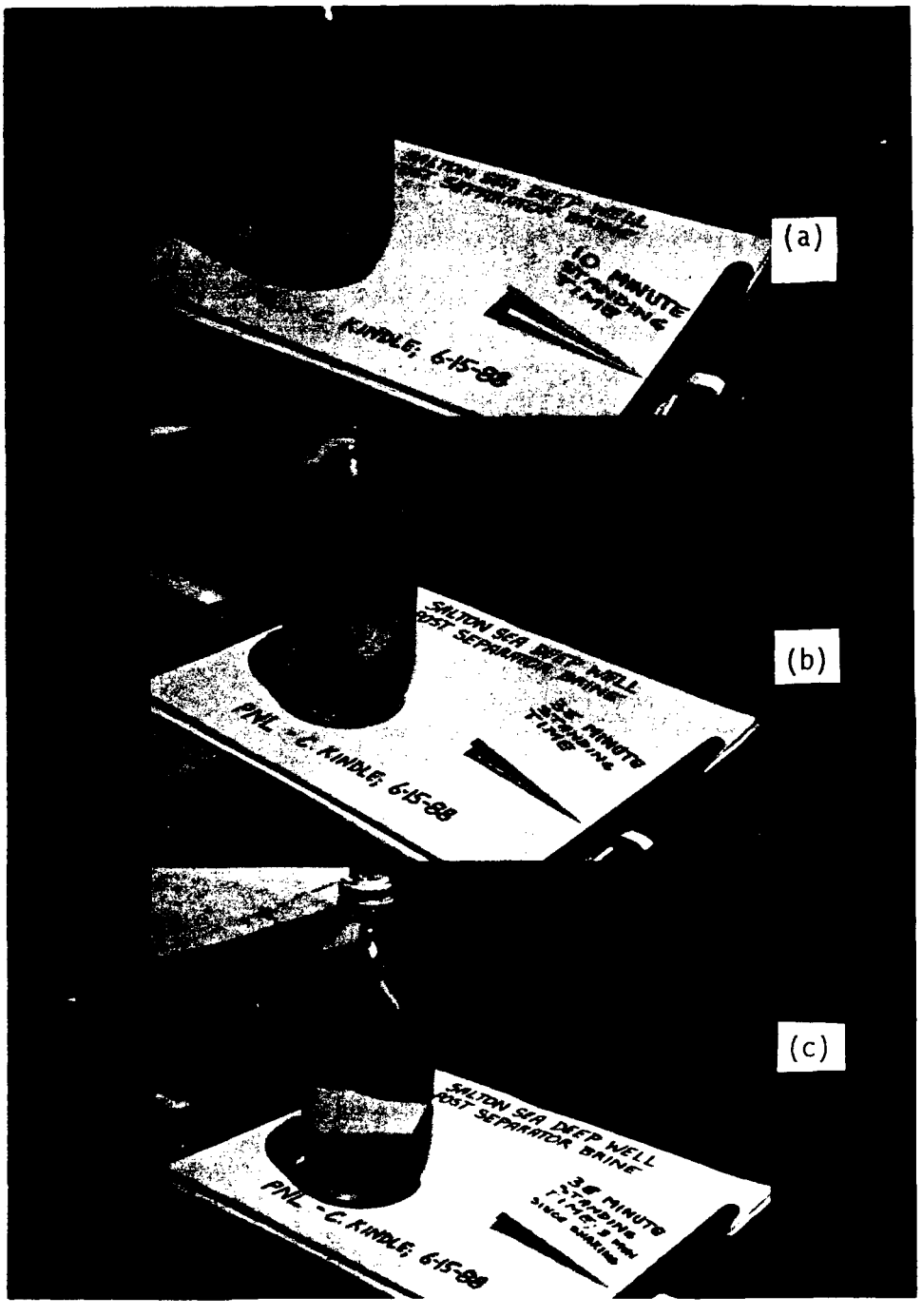

FIGURE 5.6. Sequence Showing the Rapid Formation of Precipitates (a, after 10 min) and Their Growth into Large Particles (b, shaken after 35 min) That Settle Out (c, in 3 min)

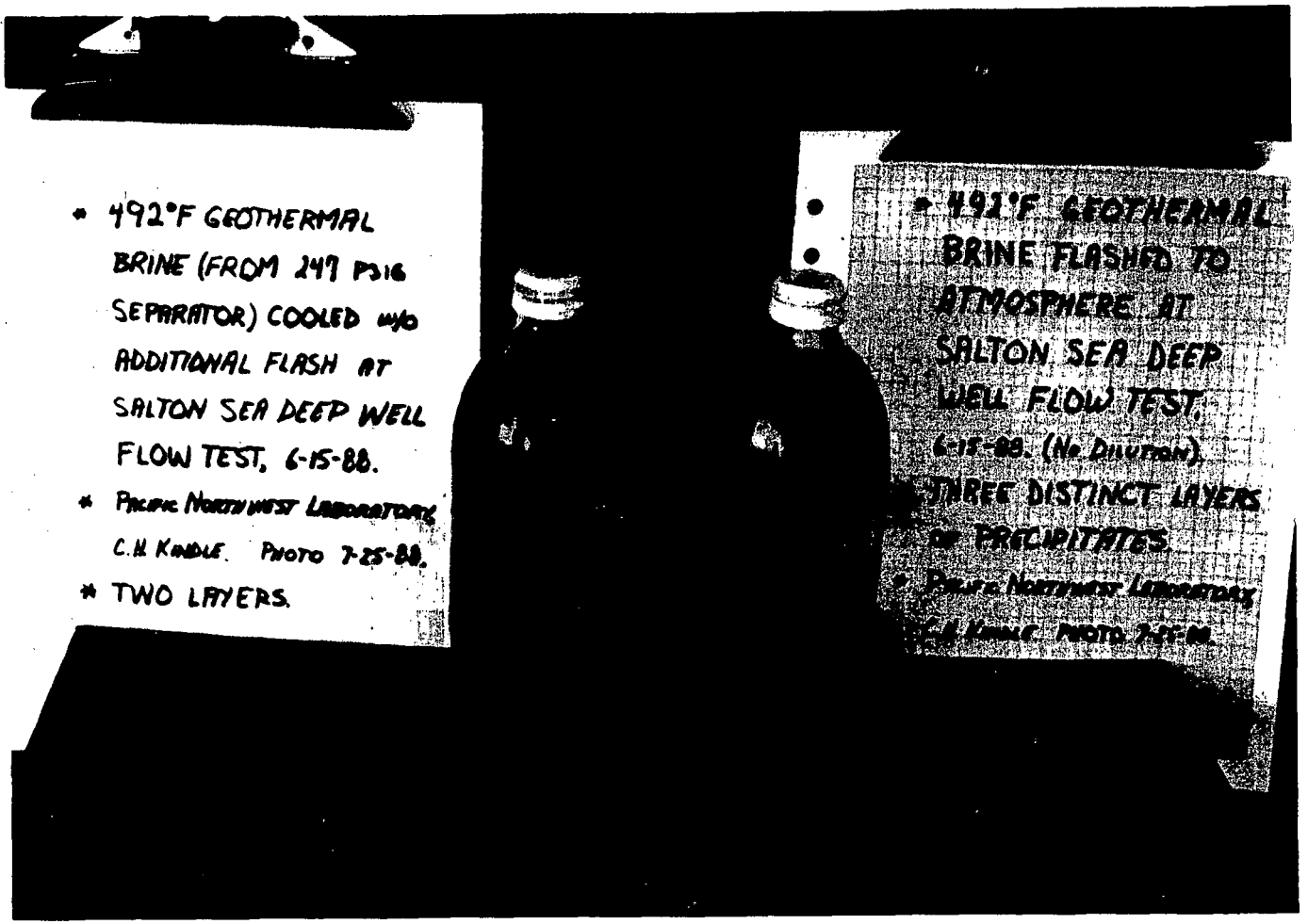

FIGURE 5.7. The Effect of Different Degrees of Flash on Brine Chemistry and the Resulting Precipitates: Separator Brine at Left was Flashed to 247 psig and Cooled Under Pressure; Brine at Right was Flashed to Atmosphere

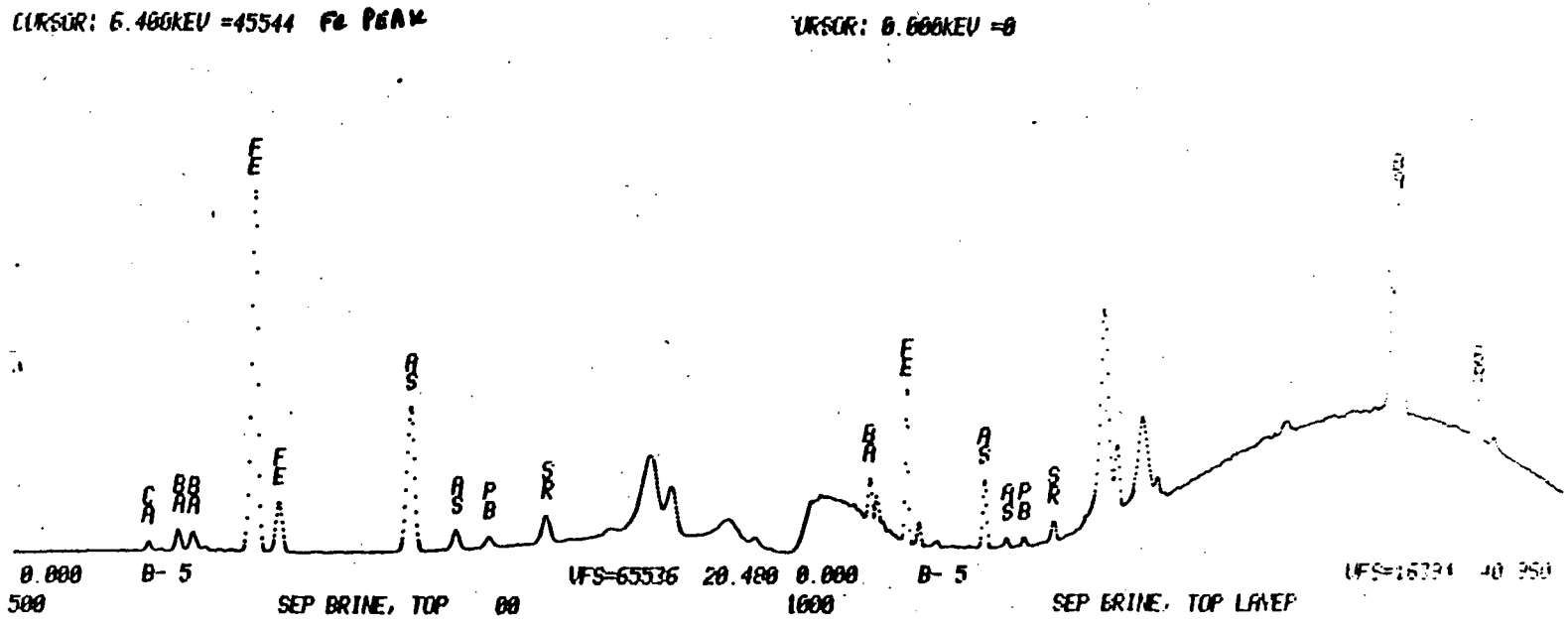

FIGURE 5.8. X-Ray Fluorescence Spectrum of the Top Precipitate Layer from the Separator Brine in Figure 5.7

read <5 ppm, which was the lower detection limit of our instrumentation. For comparison, an analysis by (SDG&E 1980) for a different well in the Salton Sea is included in the Table 5.1.

The standard deviation of the samples is reasonable, except for barium and cadmium. Since cadmium values are near the detection limits of the instrumentation, a high scatter is not surprising. Barium sulfate was identified as a major constituent in some of the filter solids samples. Since all of these brine samples were collected in similar manners and stored 1 month before analysis, similar amounts of $BaSO_4$ were expected to drop out of each one and thus similar amounts of Ba^+ to remain in solution. Exceptions are two samples that were acidified with 1 ml of concentrated HCl. The Ba^+ values for those two samples were significantly higher than the rest.

Significant amounts of amorphous silica apparently dropped out of the brine in the flash vessel piping ahead of the test stand. Further evidence was found when the test stand was disassembled. The 1/2-in. pipe connecting the test stand to the flash vessel had a thick coating of silica/salt scale inside, enough to restrict flow. The analyzed Si values for the samples were significantly below the 420 ppm SiO_2 (quartz) equilibrium values expected in the brine and reported by others (SDG&E 1980) (see Table 5.1). Consequently, those values are not reported here.

5.2.2 Solids Collection Data

Table 5.2 summarizes the solids collection data. Figure 5.9 compares weights of samples collected with an equilibrium prediction based on work by Marshal and Warakomski (1980) and Setchenow (1892). Marshal and Warakomski showed that the solubility of silica in pure water followed the empirical correlation:

$$\text{Log } s^0 = -0.1185 - (1.1260 \times 10^3/T) + (3.3\times10^5/T^2) - (3.6784\times10^7/T^3)$$

where s^0 = molal solubility of amorphous silica in pure water

T = temperature in Kelvin.

TABLE 5.2. Solids Collection Summary

Date: Location:	9-Jun-88 Inlet	10-Jun-88 Inlet 1st Run	10-Jun-88 Vessel 1st Run	10-Jun-88 Inlet 2nd Run	10-Jun-88 Vessel 2nd Run	13-Jun-88 Inlet	13-Jun-88 Lag Vessel	14-Jun-88 Inlet 1st Run	14-Jun-88 Inlet 2nd Run	15-Jun-88 Inlet	15-Jun-88 Lag Vessel
Filter °C	107	181	135	181	135	145	108	127	127	105	70
Tot min collected	5	25	39	1	10	4	51	1.75	1	9	48
Res time (min)			159		65		97				179
Tot g solids collected	0.0991	0.1693	0.9348	0.0376	0.5136	0.1023	0.5552	0.0276	0.0306	0.0503	0.3788
Meas solids (mg/kg H_2O)	347	314	421	521	602	441	166	156	242	67	115
SiO_2 ppt @ Tfilter (equilibrium prediction)	660	0	150	0	150	115	232	176	176	240	322
Solids loading (mg/kg H_2O) measured in PNL lag (1 month holding time)	1350	2880	2530			3710	1340		3590	3800	604
Total solids (expt'l)	1697	3194	2951	521	602	4161	1506	156	3832	3867	719
Equilibrium prediction at 20°C	398	398	398	398	398	398	398	398	398	398	398

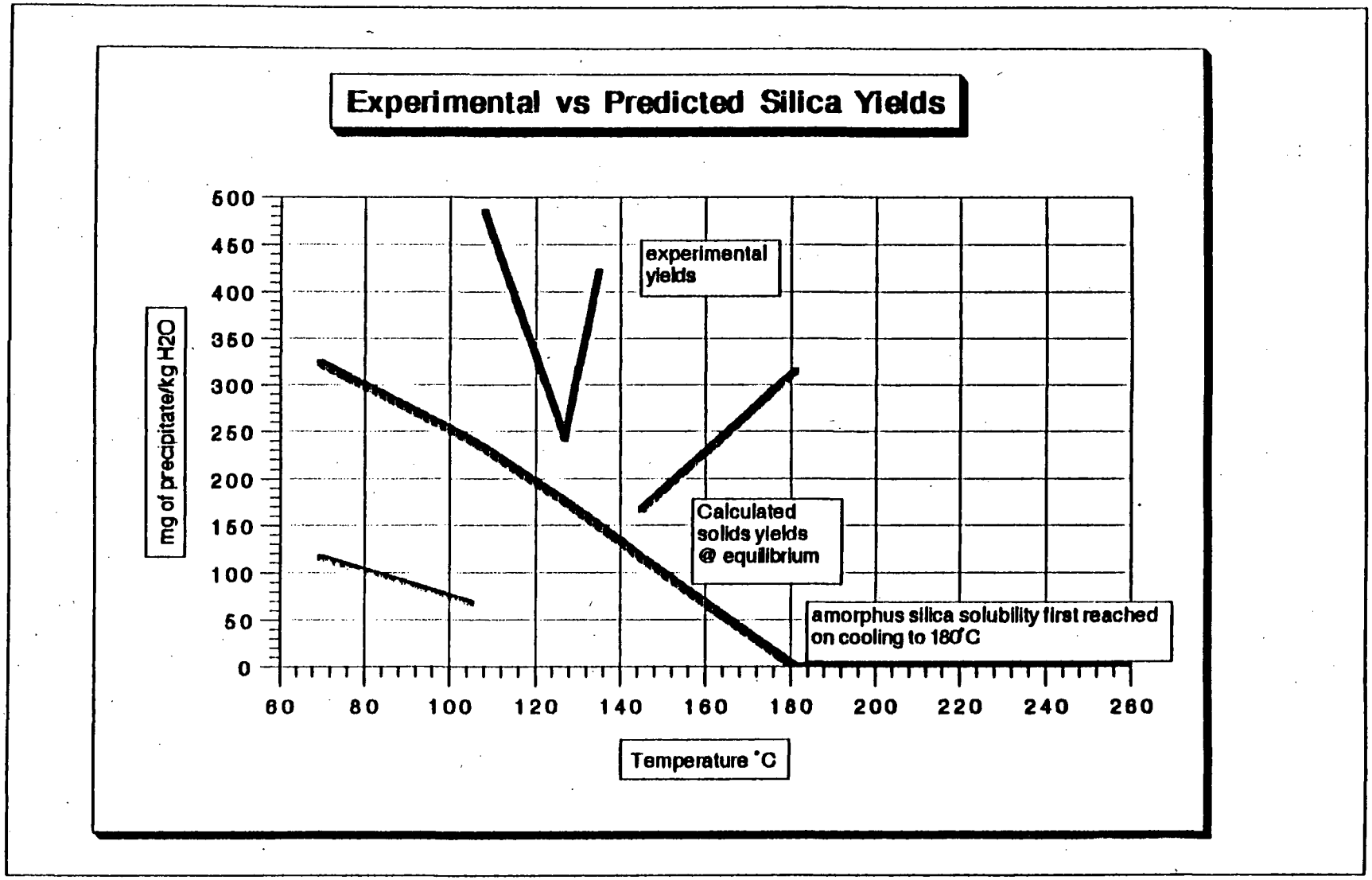

FIGURE 5.9. Experimental vs. Predicted Solids Yields

Setchenow corrected silica solubility for NaCl solutions using the now classic equation:

$$\text{Log}(s^0/s) = D\ m$$

where s = molal solubility of amorphous silica in the salt solution
D = a parameter that varies with salt type and temperature
m = molality of the added salt.

Values of D for NaCl were fitted to the equation:

$$D = 0.0874 - 2.951\text{x}10^{-4}\ T^* + 3.4326\text{x}10^{-6}\ T^{*2}$$

where T^* = temperature in °C.

Table 5.1 and Figure 5.9 use only the NaCl correction for silica solubility. Admittedly this is an oversimplification, but the calculations should at least be consistent among samples. The predicted silica yields assume that the silica in the brine is saturated with respect to quartz at the well temperature (~260°C). The quartz solubility is about 420 mg SiO_2/kg H_2O. The silica comes out of solution as amorphous silica. Generally, kinetics are slow and will determine the actual amounts formed. For this analysis, actual amounts collected are compared with equilibrium yields. The equilibrium yields represent maximum amounts to be collected at any given temperature and are independent of time.

The wide scatter in the experimental data cannot be adequately explained for all samples. The solids samples taken at the Salton Sea were washed with deionized water before being packaged and shipped to PNL for analysis. Later it was determined that the samples still contained significant amounts of NaCl deposited on the other solids. All the filters were then washed a second time with a minimum of 500 cc of distilled water. This second handling introduced errors in some samples because parts of the samples were lost during the many required transfers. Losing sample material demonstrates that we should

definitely fall below equilibrium predictions for SiO_2 yields. Since many of the samples showed greater than equilibrium yields, washing still may not have been complete.

5.2.3 Detailed Solids Analyses

All of the filter samples collected at the site were analyzed at PNL using three different techniques:

- Scanning electron microscopy (SEM) with microprobe
- X-ray diffraction (XRD)
- X-ray fluorescence (XRF).

The scanning electron microscope gave visual magnifications of the particle structure and, hence, particle size information. The microprobe gave elemental analyses for small areas down to individual particle sizes. Silicon is easily detected and is the species of most interest.

X-ray diffraction identified materials from their crystalline structure. Amorphous materials will show no identifiable pattern. The technique is not sensitive to trace amounts of materials in complex crystalline mixtures. It is most useful for identifying major crystalline compounds.

X-ray fluorescence gave elemental composition information that complemented the electron microprobe data. This technique will detect trace amounts of lead and arsenic in the presence of other highly concentrated species.

All of the filter solids showed definite similarities. Some representative information is presented in Figures 5.10 through 5.21. Figures 5.10 and 5.11 show an analysis of the solids collected in the pre-filter the first day of operation. Recall this filter was removed after the first day. The solid material was intentionally not washed before analysis. We were interested in seeing any heavy metal salts that could exist in the brine in soluble form at low temperatures. The chlorides (mostly sodium and potassium) dominate the sample. Individual particles of silica were isolated with the electron microscope. The strong iron peak in the X-ray diffraction data is believed due to metal chips from the connecting piping. The piping was still flushing itself

out when the sample was taken. The iron chips were obvious. The Ba peak on the X-ray diffraction is interesting to compare with another unwashed sample, Figure 5.16, discussed below.

Figure 5.12 attempts to reveal the crystalline structure of silica particles that were collected. Without magnification, the particle looked very amorphous, almost gelatinous, especially before complete drying. The structure shown here confirms the noncrystalline nature of the silica precipitate. Figure 5.13 shows a very high background noise (due to silica) in the X-ray diffraction trace. The Mo and Fe peaks are believed to have come mainly from metal flakes off the inlet piping. Rusty material was seen on the filter. Again Ba is conspicuous.

Figure 5.14 gives a less magnified view of some predominant silica precipitates. The Fe was detected in a particle agglomerate with no rust color. Speculation is that the iron exists as one or more silica complexes. Fe_2SiO_4 is one possibility. The X-ray diffraction pattern (Figure 5.15) also suggests FeO(OH). Ba shows up easily on the X-ray fluorescence data (Figure 5.15) but not on the X-ray diffraction or electron microprobe scans. Reasons for this are not clear.

Figure 5.16 is different from most of the other scans. This sample was scraped from the inside of the lag vessel after the unit had been shut down, drained, and cooled. The sample was unwashed and expected to be loaded with soluble chlorides. The barium sulfate crystal structure is distinctly different from the amorphous silica seen in the other SEM's. A significant difference in the X-ray diffraction scan for this sample and the pre-filter solids in Figure 5.11 is the size of the Fe peak. No rust was seen in this sample. This scan was additional evidence for believing that the Fe in Figure 5.11 was from the supply pipe. The X-ray diffraction data in Figure 5.17 are dominated by NaCl.

Figure 5.18 isolates another particle shape which appears to be an iron-silica complex. The general scan shown and several other scans (not shown) suggested the same thing. The X-ray diffraction analysis in Figure 5.19 was hampered by a small sample size. The filter was accidentally dropped prior to analysis and little material remained.

Figure 5.20 again shows the distinctive $BaSO_4$ crystals. The intermeshing with silica minerals is more obvious here than in Figure 5.16. Despite the strong presence of $BaSO_4$ in parts of the sample, the crystals were not seen with X-ray diffraction. Note, however, the high noise signal for the X-ray diffraction, which suggests high concentrations of amorphous materials (Figure 5.21). The X-ray fluorescence data would suggest contamination from the inlet piping again (Figure 5.21). There was no tell-tale rust color in this sample, however.

5.3 CONCLUSIONS

The particle counter evaluation illustrated the advantages of reflected ultrasonic impulses over laser light scattering to count suspended particles. The ultrasonic counter also generated some limited size information on the particles. The advantages included improved high-temperature durability for the transducer and improved sizing information from the reflected signal. On the other hand, laser light scattering was not practical for use in hypersaline, high-silica brines.

The brine chemistry and particulate evaluation showed the silica that formed at high temperatures and residence times is very gelatinous and difficult to filter out of the brine. Furthermore, instrument readings could not easily be correlated with particle collection data because conditions such as temperature, flowrate, and pressure could not be maintained constant on the filter for long enough intervals to obtain comparable information. The primary precipitate (by orders of magnitude) was amorphous silica. $BaSO_4$ was also identified in most precipitate samples.

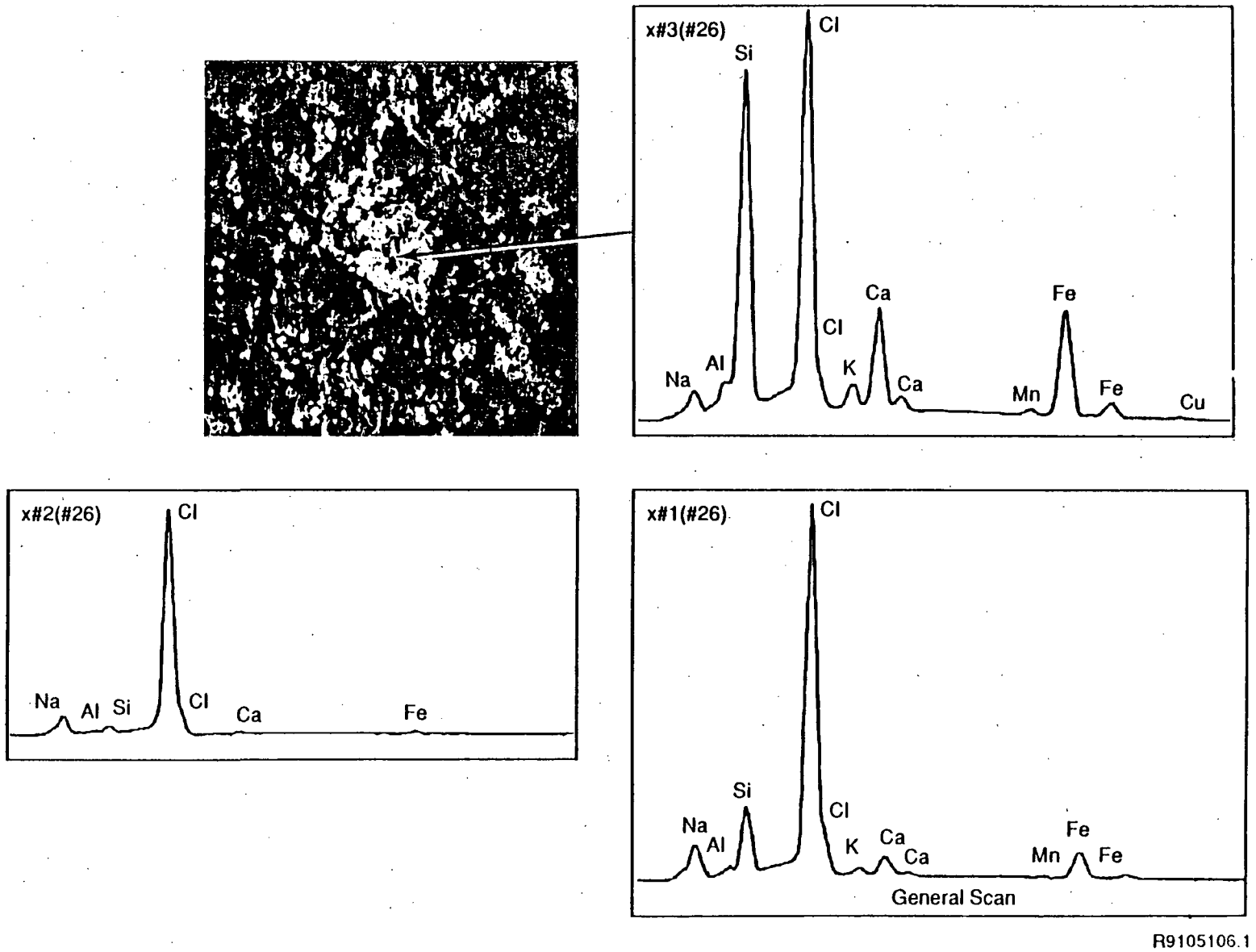

FIGURE 5.10. SEM and Microprobe Data for Prefilter Solids 9 June 88

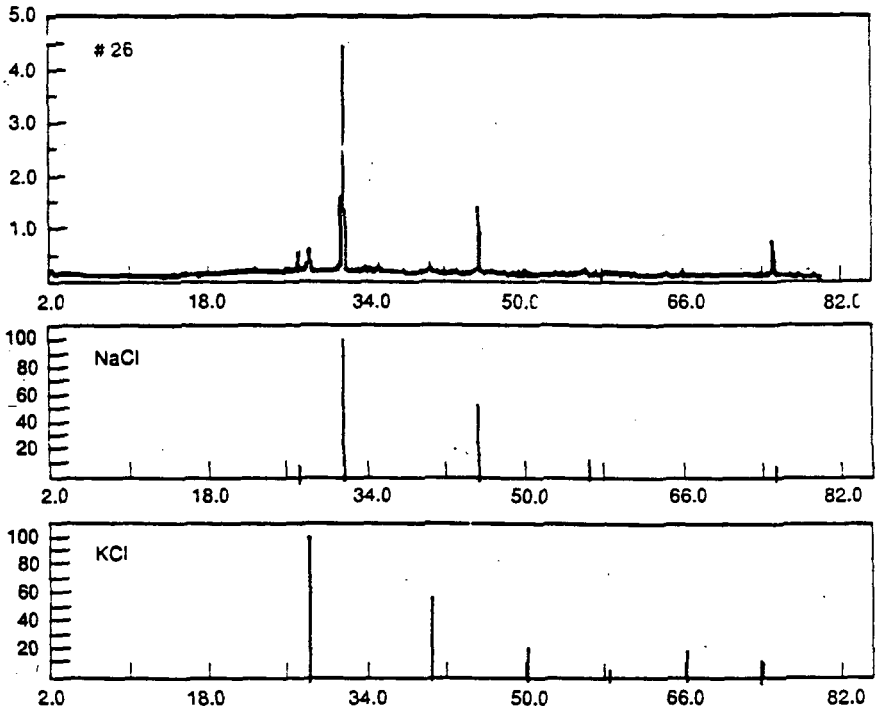

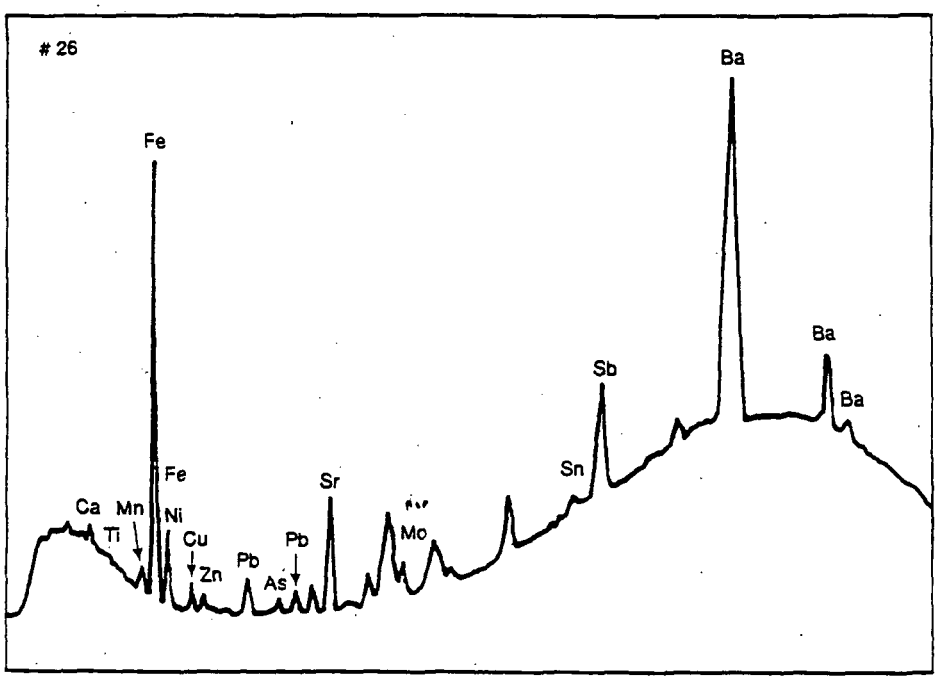

FIGURE 5.11. X-Ray Diffraction (Top) and X-Ray Fluorescence Data for Prefilter

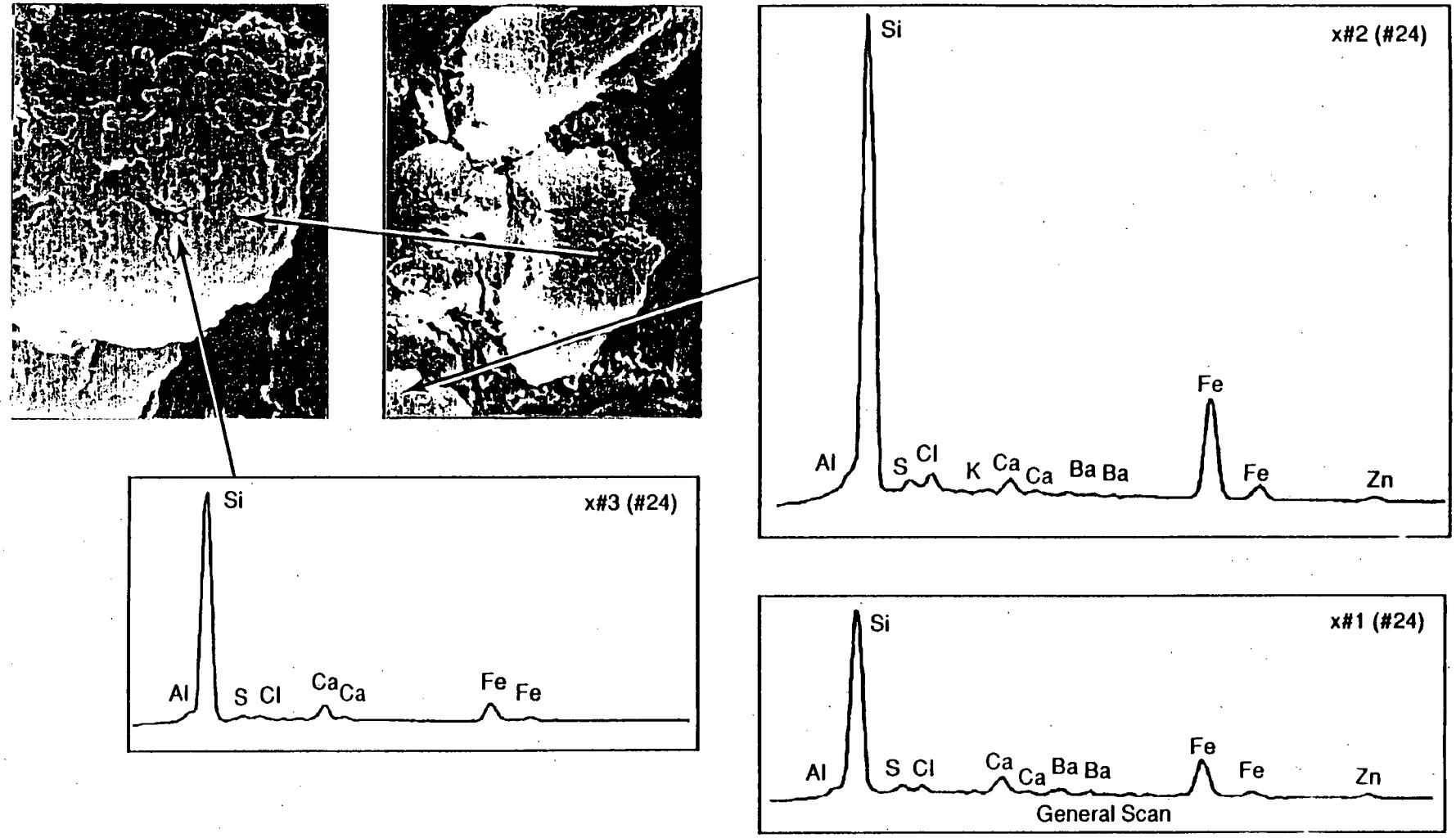

FIGURE 5.12. SEM and Microprobe Data for Solids at Inlet to Test Stand 9 June 88

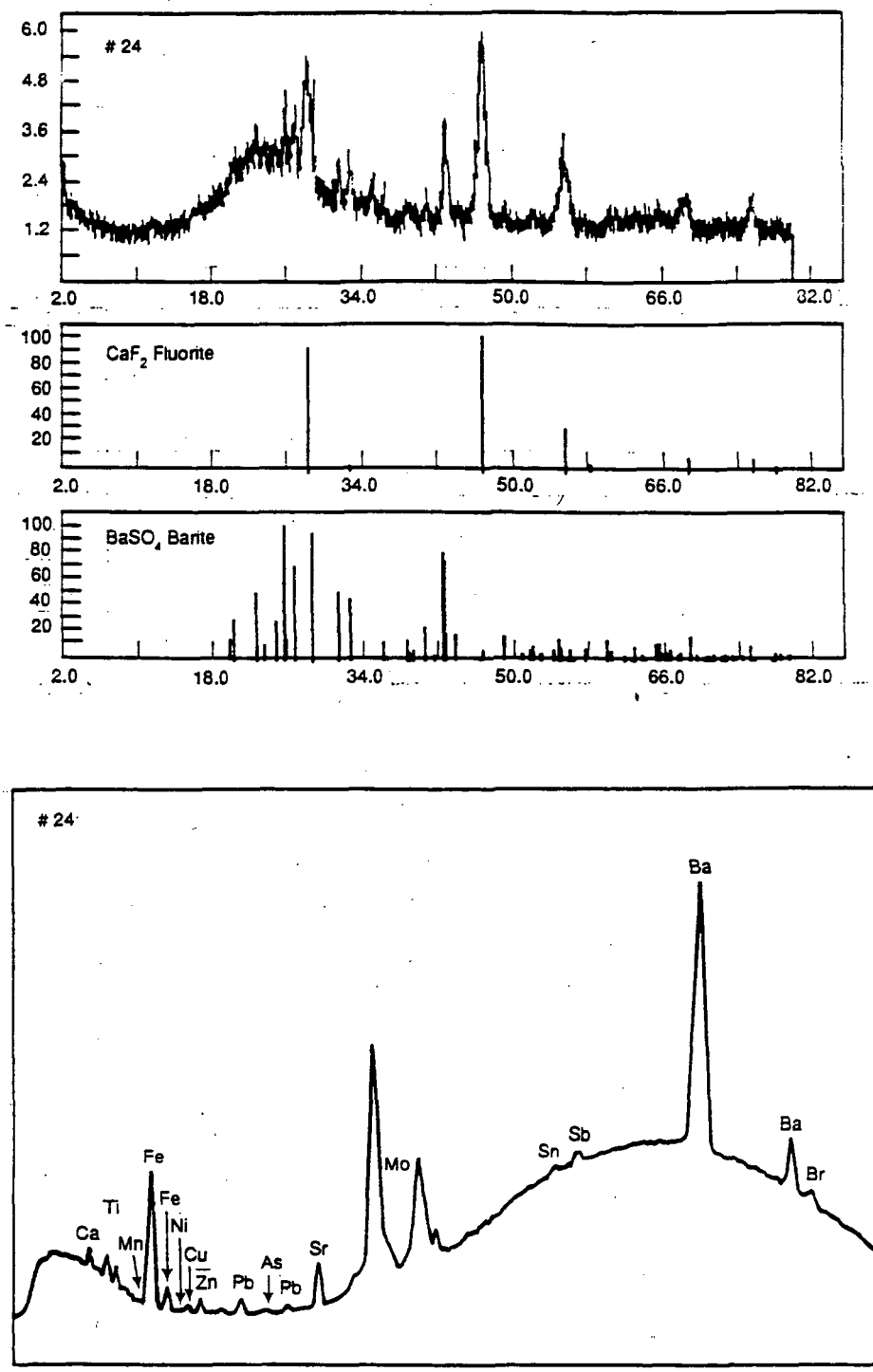

FIGURE 5.13. X-Ray Diffraction (top) and X-Ray Fluorescence Data for Solids at Inlet to Test Stand 9 June 88.

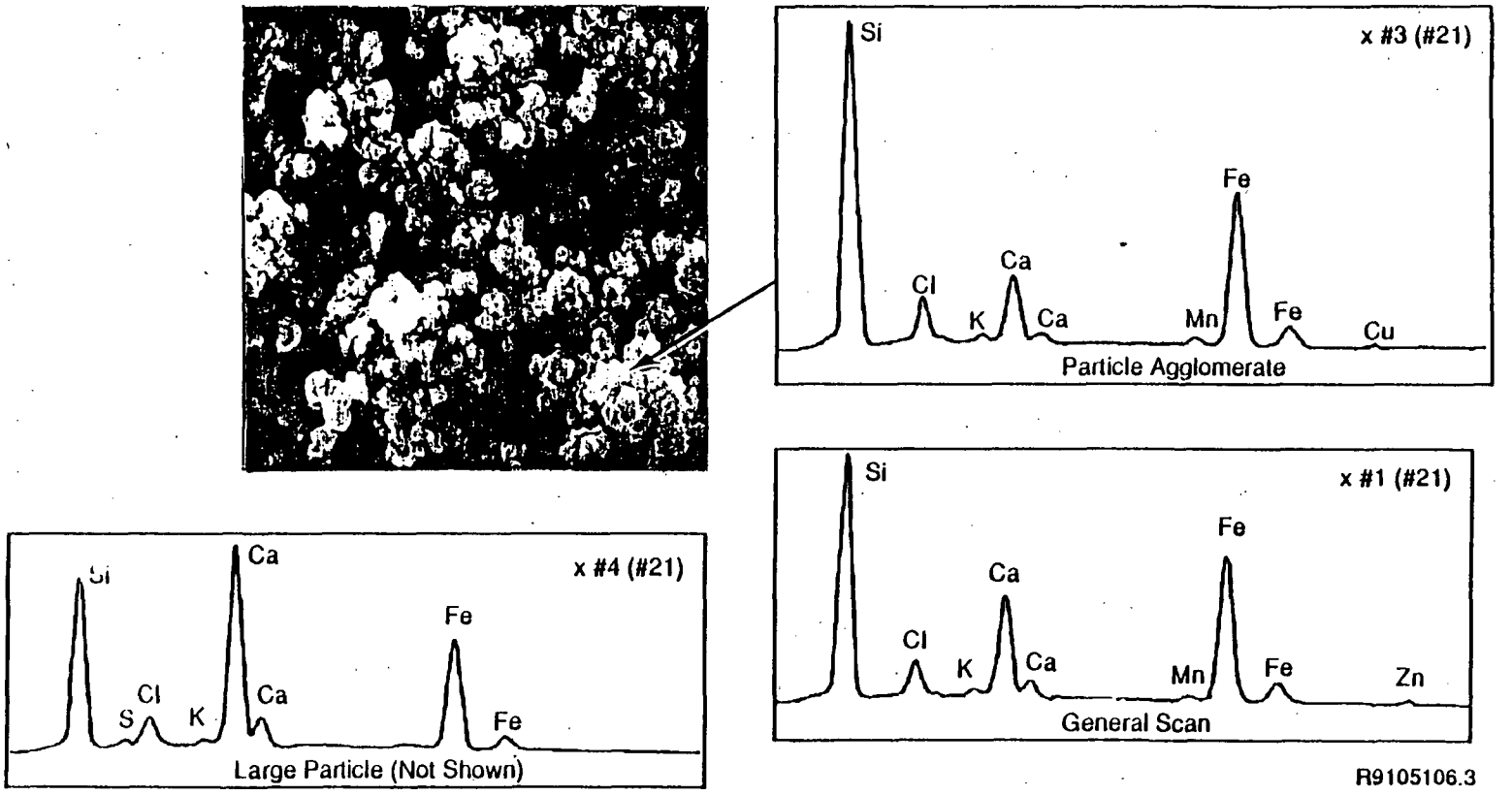

FIGURE 5.14. SEM and Microprobe Data for Solids Out the Lag Vessel 10 June 88 (Test 1)

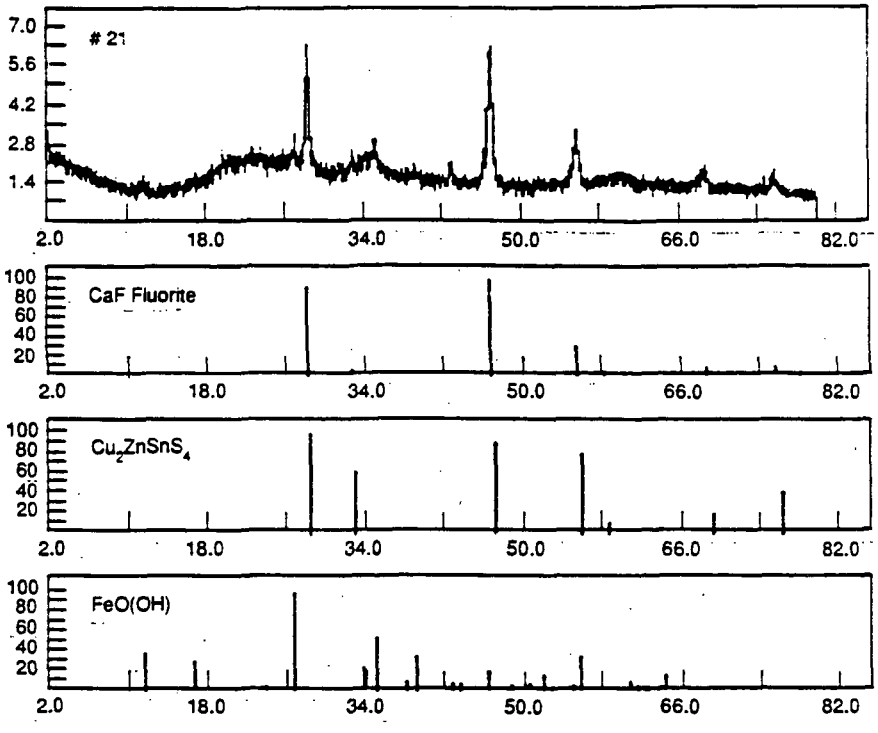

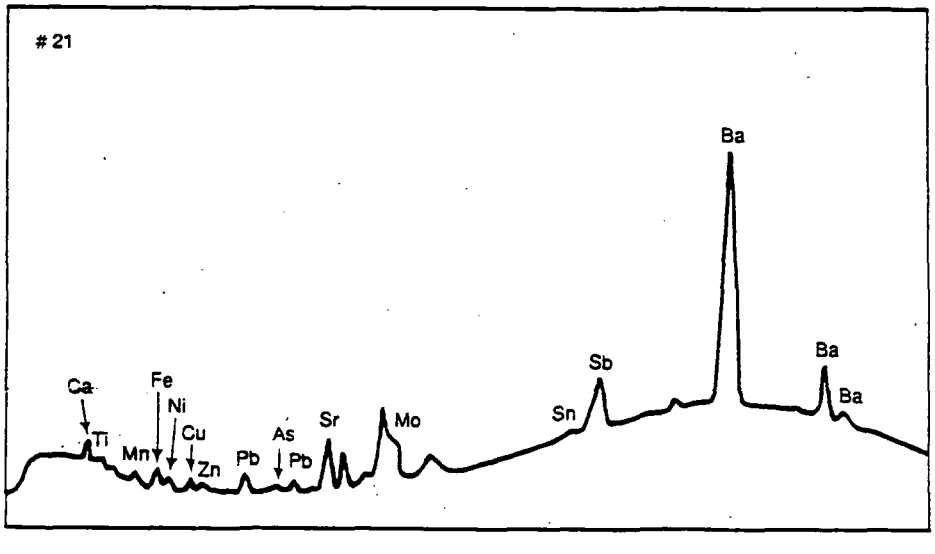

FIGURE 5.15. X-Ray Diffraction (Top) and X-Ray Fluorescence Data for Solids Out of the Lag Vessel 10 June 88 (Test 1)

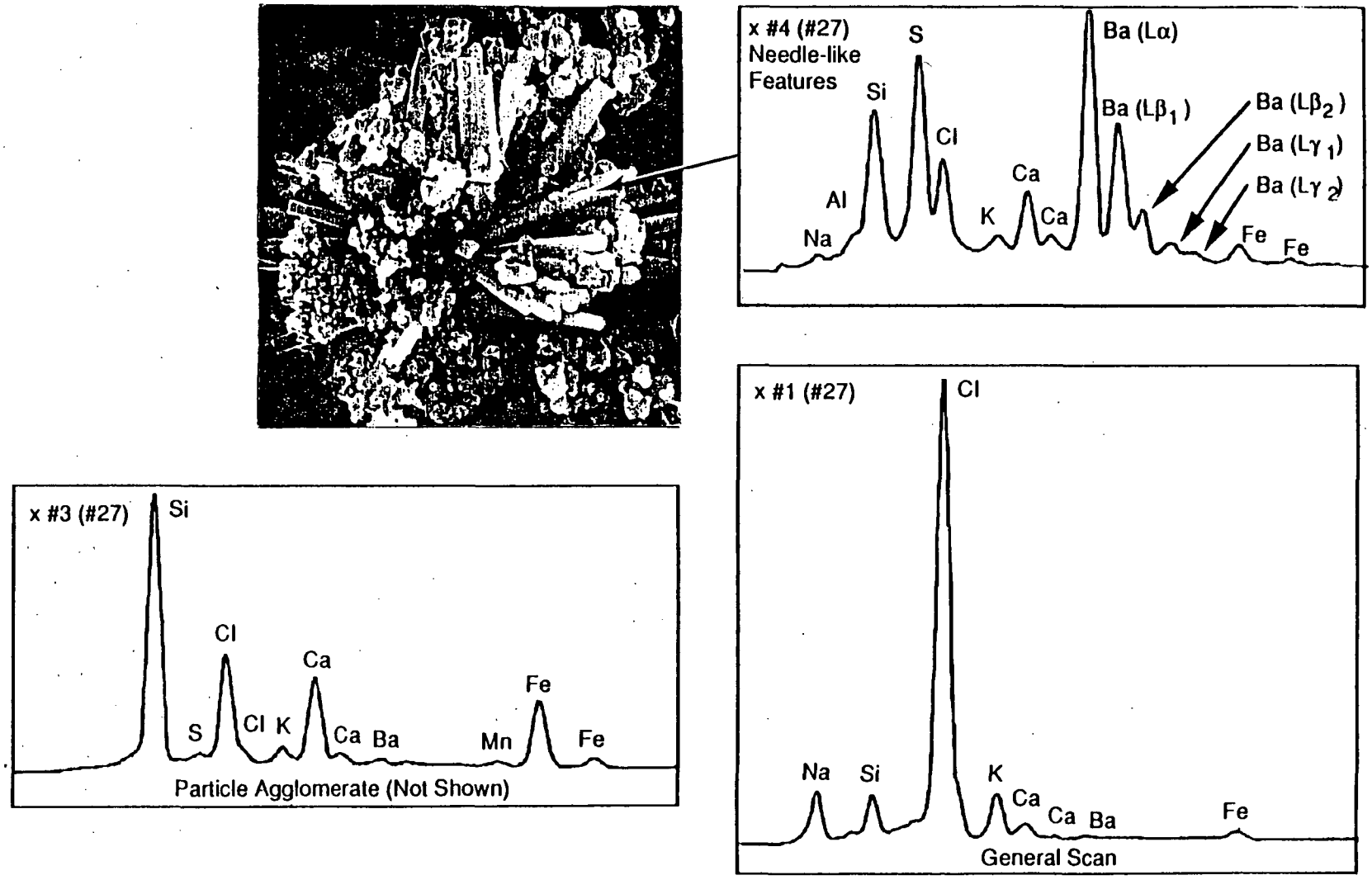

FIGURE 5.16. SEM and Microprobe Data for Solids Inside the Lag Vessel 14 June 88

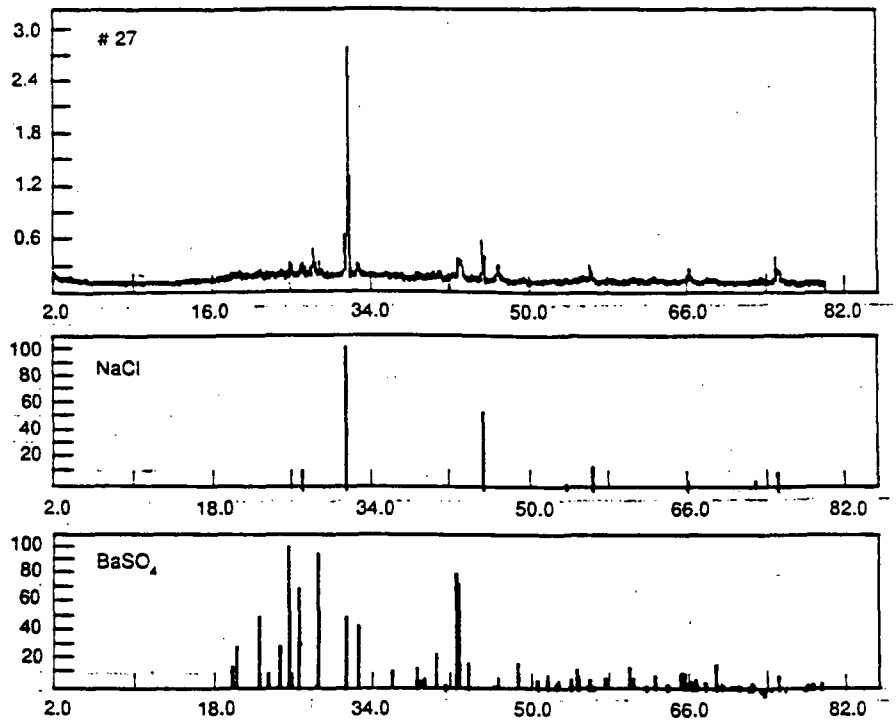

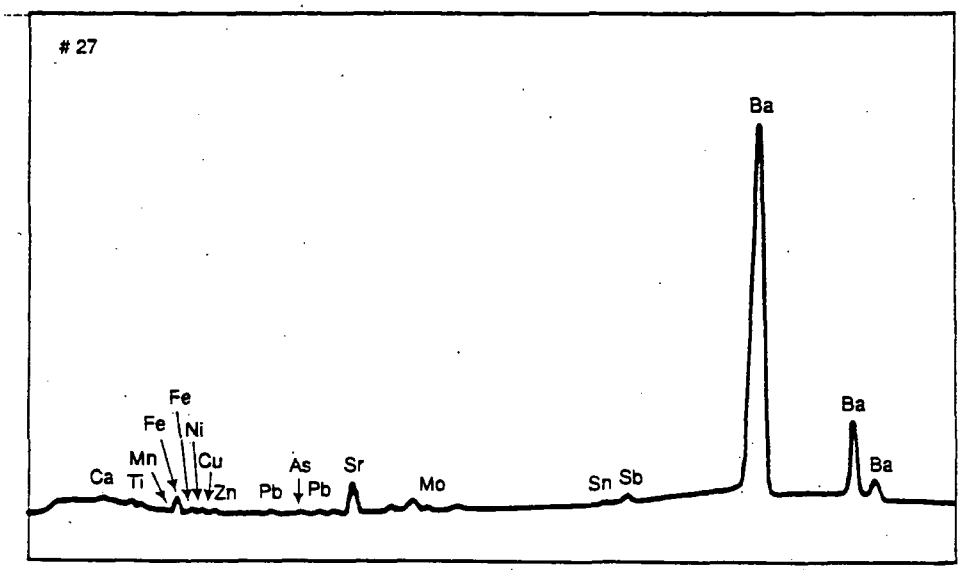

FIGURE 5.17. X-Ray Diffraction (Top) and X-Ray Fluorescence Data for Solids Inside the Lag Vessel 14 June 88

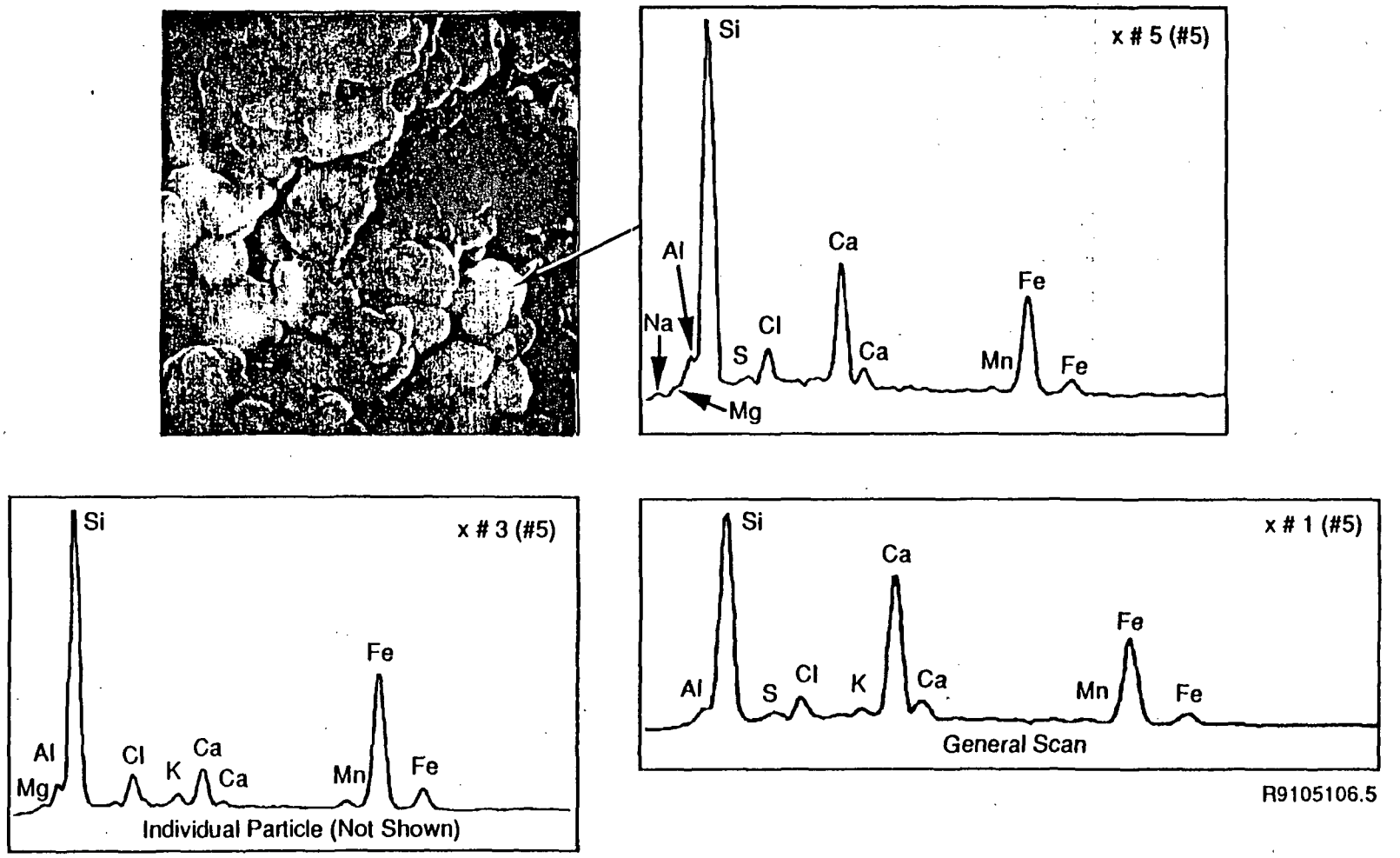

FIGURE 5.18. SEM and Microprobe Data for Solids at Test Stand Inlet 14 June 88 (Test 2)

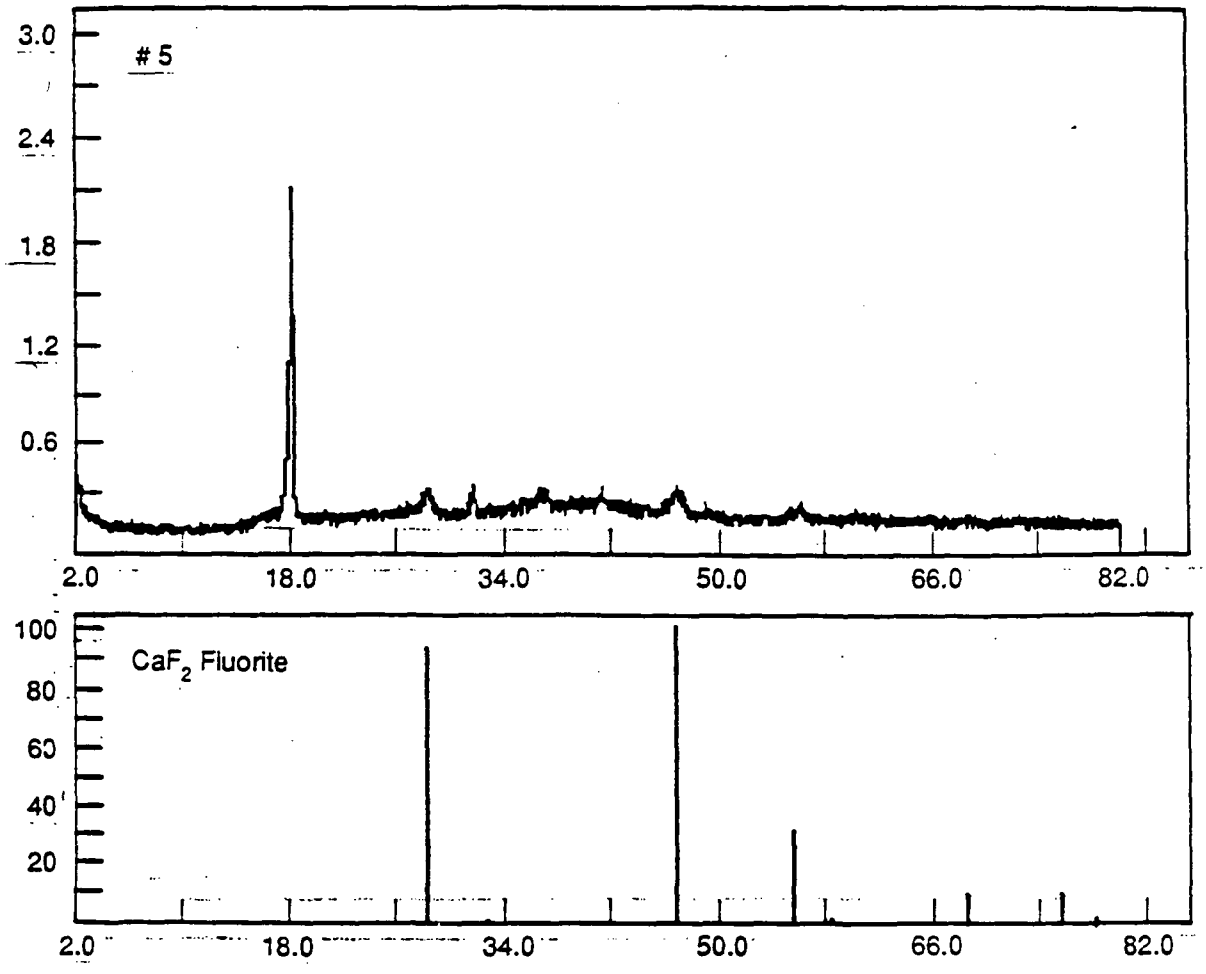

FIGURE 5.19. X-Ray Diffraction Data for Solids at Test Stand Inlet 14 June 88 (Test 2)

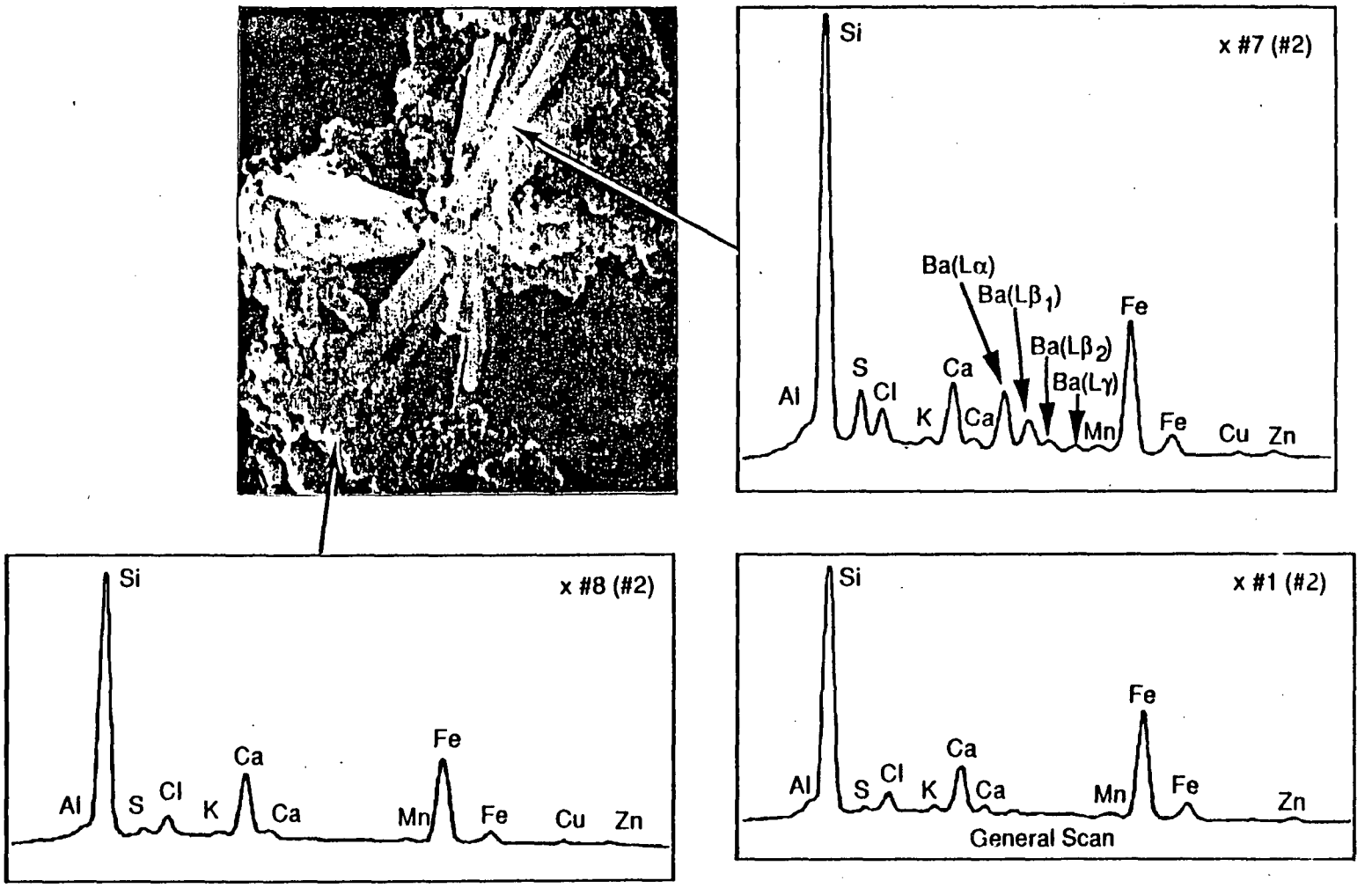

FIGURE 5.20. SEM and Microprobe Data for Solids Out the Lag Vessel 15 June 88

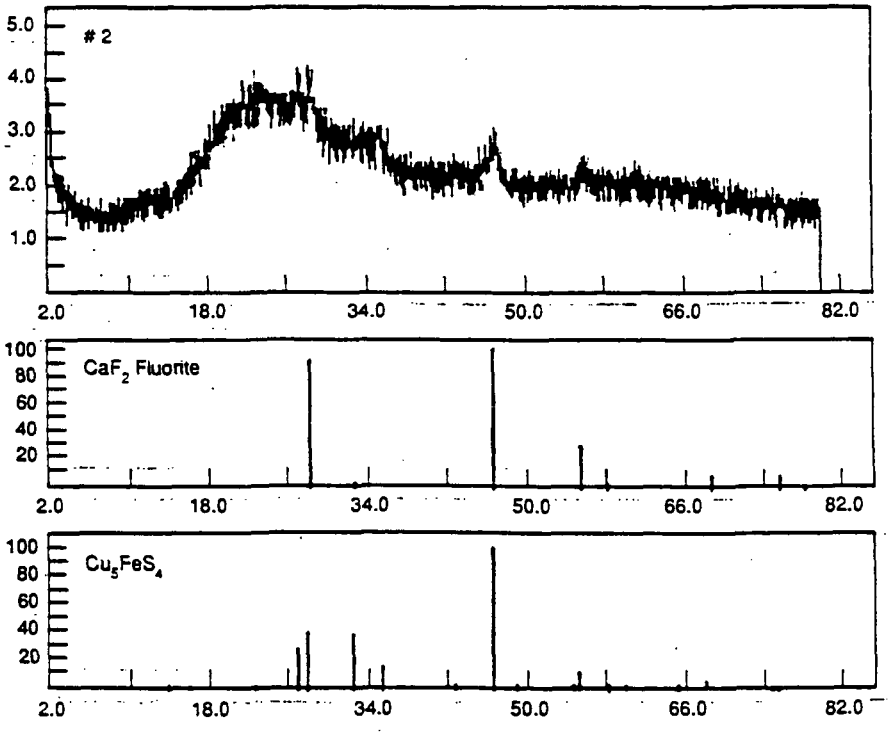

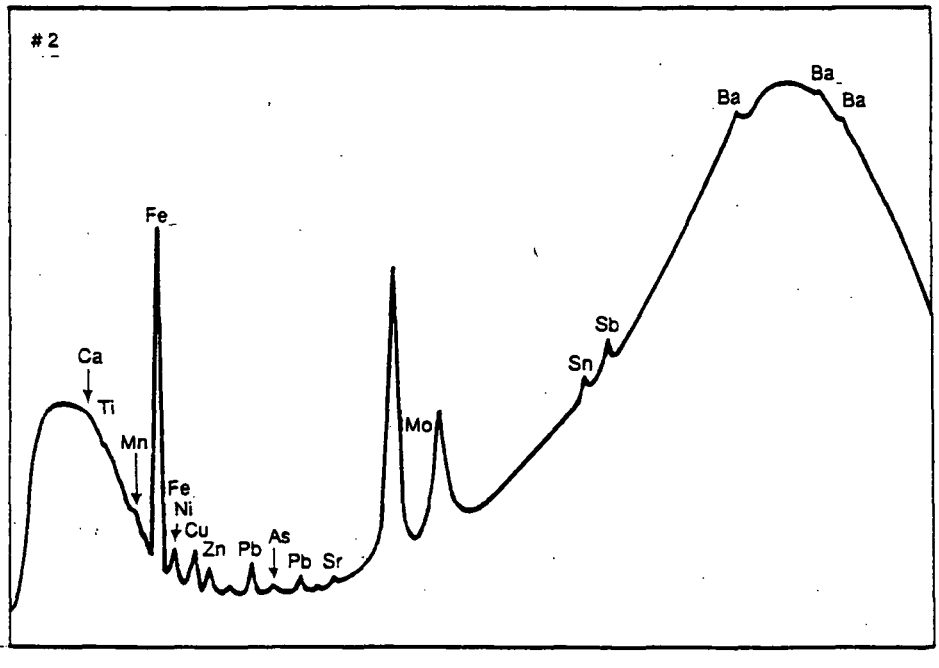

FIGURE 5.21. X-Ray Diffraction (Top) and X-Ray Fluorescence Data for Solids Out the Lag Vessel 15 June 88

6.0 REFERENCES

Marshal, W. L., and J. M. Warakomski. 1980. "Amorphous Silica Solubilities - II. Effect of Aqueous Salt Solutions at 25°C." Geochimica et Cosmochimica Acta 44:915-924.

Robertus, R. J., R. G. Sullivan, and D. W. Shannon. 1986. Field Tests to Determine Scaling Tendency of Some Moderate-Temperature Geothermal Brines. PNL-5991, Pacific Northwest Laboratory, Richland, Washington.

San Diego Gas and Electric (SDG&E). 1980. Geothermal Loop Experimental Facility - Final Report. DOE/ET/28443-T1, U.S. Department of Energy, Washington, D.C.

Setchenow, M. 1892. "Action de L'Acid Carbonique sur les Solutions des Sels a Acides Forts." Ann. Chim. Phys. 6(25):226-270.

White, D. E. 1968. "Environments of Generation of Some Base-Metal Ore Deposits." Economic Geology 63:301.

PNL-XXXX
UC-254

DISTRIBUTION

No. of Copies

OFFSITE

8 Gladys Hooper
Division of Geothermal Energy
U.S. Department of Energy
1000 Independence Ave SW
Washington, D.C. 20545

12 DOE/Office of Scientific and Technical Information

Geothermal Resources Council
P.O. Box 1350
Davis CA 95617-1350

Stu Johnson
Phillips Petroleum Co.
655 East 4500 South
Salt Lake City, UT 84107

L. Kukacka
Brookhaven National Laboratory
Upton, NY 11973

Paul Lienau
Oregon Institute of Technology
Klamath Falls, OR 97601

Technical Library
Union Oil Company of California
P.O. Box 7600
Los Angeles, CA 90017

No. of Copies

Don Thomas
Hawaii Institute of Geophysics
2525 Correa Road
Honolulu, Hawaii 96822

Victor Van Der Mast
Bechtel Group
50 Beale Street
San Francisco, CA 94105

J. H. Weare
University of California/
San Diego
LaJolla, CA 92093

ONSITE

DOE Richland Operations Office

J. J. Sutey/Don Segna

16 Pacific Northwest Laboratory

C. H. Kindle (3)
R. J. Robertus (5)
R. G. Sullivan
Technical Information (5)
Publishing Coordination (2)